Molecular Therapy
Nucleic Acids
Original Article

Protection from cisplatin-induced hearing loss with lentiviral vector-mediated ectopic expression of the anti-apoptotic protein BCL-XL

Larissa Nassauer,[1] Hinrich Staecker,[2] Peixin Huang,[2] Bryan Renslo,[2] Madeleine Goblet,[3,4] Jennifer Harre,[3,4] Athanasia Warnecke,[3,4] Juliane W. Schott,[1] Michael Morgan,[1] Melanie Galla,[1] and Axel Schambach[1,5]

[1]Institute of Experimental Hematology, Hannover Medical School, 30625 Hannover, Germany; [2]Department of Otolaryngology-Head and Neck Surgery, University of Kansas School of Medicine, Kansas City, KS 66160, USA; [3]Department of Otorhinolaryngology, Head and Neck Surgery, Hannover Medical School, 30625 Hannover, Germany; [4]Cluster of Excellence "Hearing4all", Hannover Medical School, 30625 Hannover, Germany; [5]Division of Hematology/Oncology, Boston Children's Hospital, Harvard Medical School, Boston, MA 02115, USA

Cisplatin is a highly effective chemotherapeutic agent, but it can cause sensorineural hearing loss (SNHL) in patients. Cisplatin-induced ototoxicity is closely related to the accumulation of reactive oxygen species (ROS) and subsequent death of hair cells (HCs) and spiral ganglion neurons (SGNs). Despite various strategies to combat ototoxicity, only one therapeutic agent has thus far been clinically approved. Therefore, we have developed a gene therapy concept to protect cochlear cells from cisplatin-induced toxicity. Self-inactivating lentiviral (LV) vectors were used to ectopically express various antioxidant enzymes or anti-apoptotic proteins to enhance the cellular ROS scavenging or prevent apoptosis in affected cell types. In direct comparison, anti-apoptotic proteins mediated a stronger reduction in cytotoxicity than antioxidant enzymes. Importantly, overexpression of the most promising candidate, *Bcl-xl,* achieved an up to 2.5-fold reduction in cisplatin-induced cytotoxicity in HEI-OC1 cells, phoenix auditory neurons, and primary SGN cultures. BCL-XL protected against cisplatin-mediated tissue destruction in cochlear explants. Strikingly, *in vivo* application of the LV BCL-XL vector improved hearing and increased HC survival in cisplatin-treated mice. In conclusion, we have established a preclinical gene therapy approach to protect mice from cisplatin-induced ototoxicity that has the potential to be translated to clinical use in cancer patients.

INTRODUCTION

Hearing loss is the most prevalent sensory disorder, affecting approximately 460 million people worldwide.[1] The most reported form is sensorineural hearing loss (SNHL), which is due to defects and pathological changes within the inner ear or the auditory nerve.[2] SNHL can be congenital or acquired through environmental factors such as infections, excessive noise exposure, and ototoxic drugs, including loop diuretics, aminoglycoside antibiotics, and platinum-based chemotherapeutics.[3,4] One of the most ototoxic drugs is cisplatin, a chemotherapeutic agent that is highly effective in treating solid tumors such as ovarian, testicular, or head and neck cancers.[5–8] Since its approval in 1978 by the US Food and Drug Administration (FDA) and in 1979 by the European Medicines Agency, approximately 60% of cisplatin-treated cancer patients have suffered from permanent, bilateral, and progressive tinnitus as well as high-frequency SNHL.[9–14] SNHL in these patients is characterized by dysfunction and degeneration of outer hair cells (OHCs), spiral ganglion neurons (SGNs) and the marginal cells of the *stria vascularis*.[15–17] Previous studies have demonstrated the ototoxic effect to be closely related to reactive oxygen species (ROS) accumulation and death of the affected cochlear cells.[18–23]

Several molecules that reduce cisplatin-induced ototoxicity have been identified. These molecules either supported the antioxidant defense system by increasing ROS degeneration (e.g., sodium thiosulfate, dexamethasone) or prevented cell death in affected cell types (e.g., Z-DEVD-fmk, Z-LEHD-fmk).[24–29] Although these molecules protected from cisplatin-induced ototoxicity in preclinical studies, the FDA only recently approved sodium thiosulfate as a preventive regimen. The efficacy of sodium thiosulfate was analyzed in two clinical trials (SIOPEL and COG ACCL0431) in which pediatric cancer patients received cisplatin-based chemotherapy. In these trials, patients treated with sodium thiosulfate had a 29% and 14% lower risk of hearing loss, respectively.[24,30] Despite this first success, there is a strong need for additional and novel inner ear-protective treatment options for cancer patients undergoing cisplatin treatment.

To avoid interference with cisplatin's antitumor activity at the tumor site, ototoxicity-preventing drugs should ideally be applied locally via

Received 13 September 2023; accepted 15 February 2024;
https://doi.org/10.1016/j.omtn.2024.102157.

Correspondence: Melanie Galla, PhD, Institute of Experimental Hematology, Hannover Medical School, Carl-Neuberg-Strasse 1, 30625 Hannover, Germany.
E-mail: galla.melanie@mh-hannover.de
Correspondence: Axel Schambach, MD, PhD, Institute of Experimental Hematology, Hannover Medical School, Carl-Neuberg-Strasse 1, 30625 Hannover, Germany.
E-mail: schambach.axel@mh-hannover.de

intratympanic or intracochlear administration.[31–34] However, since chemotherapy often involves several cycles of treatment, repeated administration of antiototoxic drugs is required, which is invasive and could cause adverse local reactions, such as inflammation.[35] Furthermore, the short half-life of antiototoxic drugs ranging from 15 min to 5.5 h could limit the therapeutic effect within the cochlea.[36,37]

Therefore, viral vector-based gene therapy approaches appear to be a promising alternative, with a single administration of the vector ensuring long-term and high-level expression of the protective transgene. Among different vector platforms, in particular, lentiviral (LV) vectors can be pseudotyped to specifically target the cells of interest and can be highly concentrated to increase titers.[38] The latter is especially important for local application to the inner ear because the injection volume is very limited due to the bony structure of the cochlea, leading to hydraulic trauma if larger volumes are introduced.[39] Moreover, previous studies showed that local injection of LV vectors into the inner ear elicited only mild immune responses, and the vector did not spread to the brain or other organs.[40] Also, LV vector administration did not negatively affect hearing because functional testing revealed no altered auditory brainstem response (ABR).[41]

To protect cochlear cells from cisplatin-induced toxicity, we therefore developed a gene therapy strategy based on third-generation self-inactivating (SIN) LV vectors. To counteract cisplatin-mediated ROS generation and/or apoptosis induction, we equipped the LV vectors with gene expression cassettes for ectopic expression of the antioxidant enzymes superoxide dismutase 1 (*SOD1*), catalase (*CAT*), or glutathione peroxidase (*GPX1*), or the anti-apoptotic proteins B cell lymphoma 2 (*BCL-2*) or B cell lymphoma-extra large (*Bcl-xl*), respectively. We first tested their anti-ototoxic potential *in vitro* using House Ear Institute-organ of Corti 1 (HEI-OC1) cells and found that ectopic expression of the anti-apoptotic proteins BCL-2 and BCL-XL, but not of the antioxidant enzymes SOD1, CAT, or GPX1, significantly reduced the toxic effects of cisplatin. Subsequently, the most potent candidate from the studies in HEI-OC1 cells, *Bcl-xl*, also showed beneficial effects in phoenix auditory neurons, primary SGN, and HCs in primary explant cultures. Importantly, LV expression of *Bcl-xl* improved hearing and decreased OHC loss in a mouse model of cisplatin-induced hearing loss.

RESULTS

Cisplatin significantly increases ROS generation and leads to cumulative cytotoxicity in HEI-OC1 cells

To assess the cellular and molecular mechanisms involved in cisplatin-mediated ototoxicity, we used the inner ear cell line HEI-OC1, which is derived from the auditory organ of the Immortomouse. HEI-OC1 cells express specific markers of cochlear HCs and supporting cells and were reported to be sensitive to ototoxic drugs, including cisplatin.[42] Testing different concentrations of cisplatin in HEI-OC1 cells, Kalinec *et al.* demonstrated a dose-dependent decrease in viability and an increase in cytotoxicity.[42,43] Since then, different cisplatin concentrations have been applied to study the cytotoxic effects of cisplatin in HEI-OC1 cells.[44–46] Thus, to find an appropriate dose for our experiments, we first tested different cisplatin concentrations in HEI-OC1 cells and analyzed the cultures for signs of cytotoxicity (Figure S1). Cisplatin-mediated cytotoxicity was first assessed by the ApoTox-Glo Triplex assay, which allows the simultaneous analysis of cell death and caspase-3/-7 activity in treated cultures. The assay revealed increased dead-cell protease (Figure S1A) and caspase-3/-7 activity (Figure S1B) in HEI-OC1 cells upon increasing cisplatin doses. Furthermore, a significant increase in Annexin V^+/$DAPI^+$ cells was observed upon 72 h of cisplatin treatment at all of the concentrations tested (Figure S1C). Since 5 μM cisplatin already caused significant differences in caspase-3/-7 activity and cell death compared to untreated cells, and in addition, a concentration of 5 μM cisplatin was observed in the *scala tympani* of guinea pigs in an *in vivo* study, HEI-OC1 cells were treated with 5 μM cisplatin for 72 h in all further experiments.[47]

To analyze whether HEI-OC1 cells are a suitable cell model to test our antiototoxic strategy, we next performed different assays in which the toxic effects of cisplatin were characterized (Figure 1). Total cell numbers decreased from 8.5×10^5 to 4.8×10^5 cells upon incubation with cisplatin, revealing a ∼1.8-fold reduction (Figure 1A). In line with the literature, cisplatin-treated HEI-OC1 cultures also showed significantly elevated ROS levels as compared to their nontreated counterparts (Figure 1B).[48–50] Furthermore, cell death was indicated by a 3.3-fold increase (from 0.23 to 0.77 relative protease activity) in dead-cell protease activity (Figure 1C). Because different cell death pathways exist, we further elucidated the mechanism of cisplatin toxicity. Although previous studies report that cisplatin induces different cell death pathways, most propose a form of programmed cell death (PCD), including apoptosis. We observed significantly increased caspase-3/-7 activity (Figure 1D) and significantly elevated Annexin V^+ percentages upon 2, 4, 8, and 48 h cisplatin treatment (Figure 1E). Because caspase-3 is involved in PCD pathways and Annexin V positivity is a hallmark of early apoptosis, our experiments also support that cisplatin treatment evokes PCD, and in particular, apoptosis.[51,52]

In summary, the destructive effect of cisplatin treatment in HEI-OC1 cells was confirmed in our experimental setting. In this cell model, 5 μM cisplatin applied for 72 h significantly increased ROS generation and induced a form of PCD, including apoptosis. Therefore, HEI-OC1 cells represent a suitable test system to analyze protective strategies for the prevention of cisplatin-mediated cytotoxicity in otic cells.

Ectopic expression of the antioxidant enzymes *SOD1*, *CAT*, or *GPX1* does not combat cisplatin-mediated cytotoxicity in HEI-OC1 cells

Since treatment with cisplatin created an oxidative stress condition with increased ROS levels (Figure 1B) and was reported to decrease the expression or activation of antioxidant enzymes in cochlear cells, we hypothesized that the ectopic expression of antioxidant enzymes

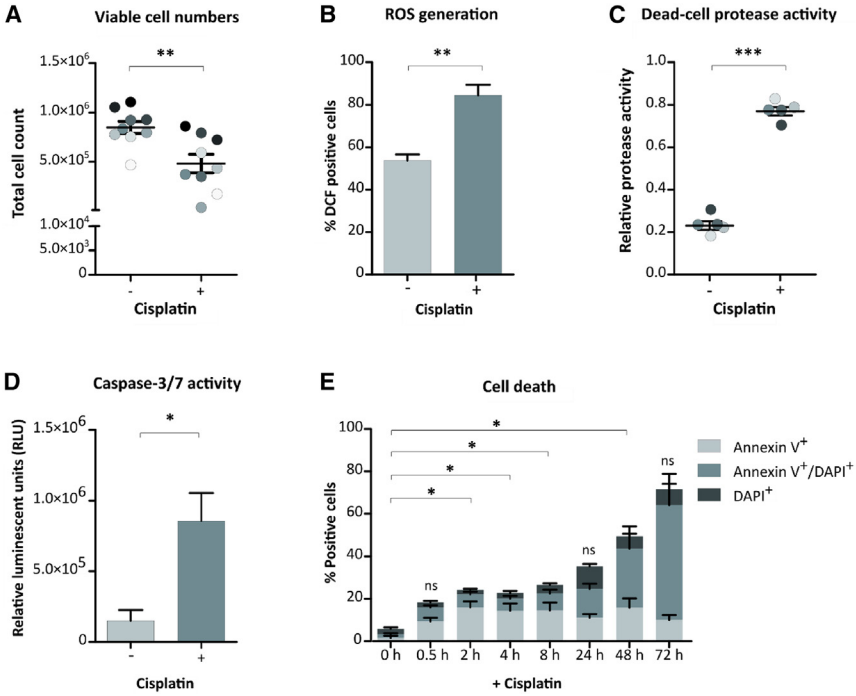

Figure 1. Cisplatin exerts cytotoxic effects in HEI-OC1 cells

HEI-OC1 cells were cultured in the presence (+) or absence (–) of 5 μM cisplatin and analyzed for cisplatin-mediated cytotoxicity after 72 h of incubation.

(A) The total viable cell numbers of cisplatin-treated and untreated HEI-OC1 cells were assessed by flow cytometry after initially seeding 5×10^4 HEI-OC1 cells for each sample. N = 9 independent experiments. (B) For the detection of ROS generation, HEI-OC1 cells were incubated with the H_2DCFDA probe, which is converted to the highly fluorescent DCF in the presence of ROS. The graph depicts the percentage of DCF^+ cells. N = 3 independent experiments. (C) Detection of the relative dead-cell protease activity via ApoTox-Glo Triplex Assay. N = 5 individual experiments. Each color indicates an individual experiment. (D) The ApoTox-Glo Triplex Assay measured caspase-3/-7 activity in the form of RLUs to quantify HEI-OC1 cells that died by PCD. N = 3 independent experiments. (E) Annexin V and DAPI co-staining of HEI-OC1 cells to analyze the proportion of early apoptotic (Annexin V^+/$DAPI^-$), late apoptotic (Annexin V^+/$DAPI^+$), or dead ($DAPI^+$/Annexin V^- or Annexin V^+/$DAPI^+$) cells in cisplatin-treated cultures. N = 3 individual experiments. Statistical analysis was conducted to assess disparities in Annexin V^+ cells from the 0 h time point to subsequent time points postcisplatin treatment, using one-way ANOVA along with Dunnett's post hoc test (*$p \leq 0.05$; ns, not significant). The data in (A)–(D) are presented as mean ± SD (*$p \leq 0.05$; **$p \leq 0.01$; and ***$p \leq 0.001$, determined using an independent t test).

could decrease the elevated ROS levels and thus increase cell survival upon cisplatin treatment.[53] To test this hypothesis, HEI-OC1 cells were engineered to overexpress human codon-optimized *SOD1*, *CAT*, or *GPX1* from SIN LV vectors (Figure 2A). The selected enzymes are among the most abundant antioxidant enzymes in the cochlea and work together to detoxify ROS.[54,55] While SOD1 reduces ROS to hydrogen peroxide (H_2O_2),[55] both CAT and GPX1 can further reduce H_2O_2 to water and thus minimize oxidative stress within a cell (Figure S2A).[56,57]

To monitor gene expression or select transduced cells *in vitro*, vectors were equipped with a reporter. For this, SIN LV vectors are commonly designed to coexpress a fluorescent protein (most commonly enhanced green fluorescent protein [EGFP]), or an antibiotic resistance gene, such as the puromycin resistance (PuroR) gene. However, since it was reported that EGFP expression could decrease the toxicity of platinum-containing chemotherapeutic agents, including cisplatin, we first tested two vector control (VC) configurations devoid of any antioxidant enzyme gene, carrying either EGFP or PuroR only (Figure S2B, top).[58] As the VC expressing EGFP reduced the percentages of annexin V^+/$DAPI^+$ HEI-OC1 cells upon cisplatin treatment (Figure S2B, bottom), the SIN LV vector carrying the PuroR gene was selected as a neutral VC and to be coexpressed from the therapeutic vectors.

HEI-OC1 cells were transduced with the SIN LV vectors coexpressing *SOD1*, *CAT*, or *GPX1* and PuroR, or with the VC (Figure 2A). Western blot analysis confirmed ectopic protein expression of the antioxidant enzymes in puromycin-treated cultures (Figure 2B) and was followed by analysis of enzyme functionality. To investigate the enzymatic activity of SOD1, non-transduced cells (NTCs) and LV.SOD1-overexpressing HEI-OC1 cultures were subjected to cisplatin treatment and analyzed for their ability to convert ROS to H_2O_2 (Figure 2C). In contrast to NTCs (78.65% SOD1 activity in untreated sample), LV.SOD1-overexpressing cells showed slightly increased SOD1 activities in untreated (91.45%) and cisplatin-treated (106.12%) conditions. The functionality of CAT and GPX1 expressed in HEI-OC1 cells was tested by determining the rescue from H_2O_2-induced toxicity as compared to non-modified and VC HEI-OC1 cells, which revealed reduced percentages of both Annexin V^+ and Annexin V^+/$DAPI^+$ cells upon LV.GPX1 and especially LV.CAT overexpression (Figure 2D). Thus, LV.GPX1 and LV.CAT overexpression reduced cell death rates, indicating that they actively detoxified H_2O_2 in the treated cells.

Finally, we assessed the effect of LV.SOD1, LV.CAT, and LV.GPX1 in terms of protection from cisplatin toxicity by analyzing ROS generation upon cisplatin administration (Figure 2E). However, ectopic expression of the antioxidant enzymes failed to significantly reduce cisplatin-induced ROS production. Next, we determined the percentage of dead cells in cisplatin-treated cultures and again were unable to detect a significant protective effect of LV.SOD1, LV.CAT, or LV.GPX1 (Figure 2F). In line with this, dead-cell protease (Figure S2C) and caspase-3/-7 activities (Figure S2D) were not decreased

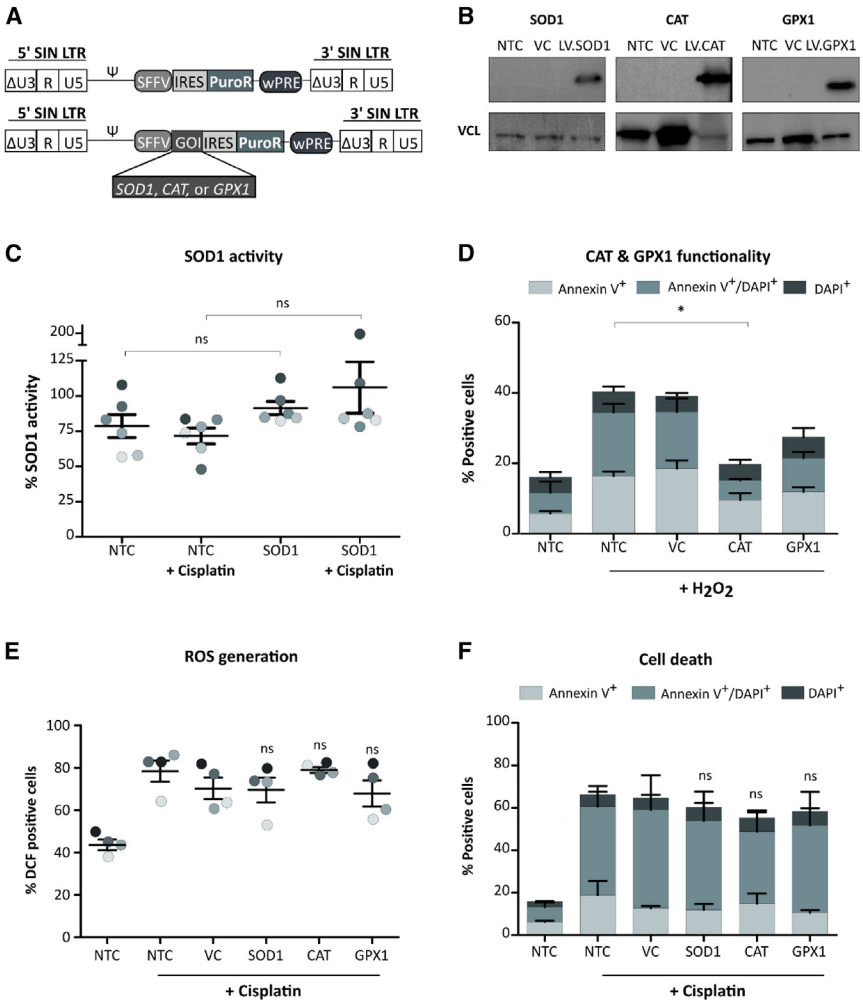

Figure 2. Ectopic expression of LV.SOD1, LV.CAT, or LV.GPX1 does not increase the survival of cisplatin-treated HEI-OC1 cells

(A) SIN LV vector design in a postintegration configuration. The deletion of U3 promoter/enhancer sequences (ΔU3) within the long terminal repeats (LTRs) results in transcriptional inactivation of the LTR and attenuates or even prevents the aberrant activation of nearby genes (SIN design). Expression of the GOIs, such as human codon-optimized *SOD1*, *CAT*, or *GPX1*, is driven by the promoter from the spleen focus-forming virus (SFFV). All of the vectors coexpressed the puromycin resistance (PuroR) gene via an internal ribosomal entry site (IRES) sequence to select for transduced cells. A vector only carrying PuroR (VC) served as transduction control. ψ, packaging signal; wPRE, woodchuck hepatitis virus posttranscriptional regulatory element; ΔU3/R/U5, regions of the SIN LV LTR. (B) Representative western blot demonstrating the ectopic expression of human SOD1 (16 kDa), CAT (60 kDa), and GPX1 (24 kDa) from SIN LV vector constructs in transduced (LV) HEI-OC1 cells as compared to non-transduced cells (NTCs) and the VC. Endogenous vinculin (VCL;116 kDa) expression served as a loading control. (C) SOD functionality in untreated and cisplatin-treated (5 μM, 72 h) HEI-OC1 cells determined using the Superoxide Dismutase Activity Assay. (D) The functionality of CAT and GPX1 was investigated by H_2O_2 treatment (500 μM, 48 h) and subsequent cell death analysis, determining the percentage of Annexin V^+, Annexin V^+/$DAPI^+$, and $DAPI^+$ cells. (E) ROS levels in cisplatin-treated (5 μM, 72 h) HEI-OC1 cells assessed by staining with H_2DCFDA as DCF^+ cells generated in the presence of ROS. For statistical analysis, samples were compared to cisplatin-treated NTCs. (F) Proportion of Annexin V^+, Annexin V^+/$DAPI^+$, and $DAPI^+$ cells in the indicated HEI-OC1 cultures after cisplatin (5 μM, 72 h) treatment. Each group is compared to cisplatin-treated NTCs in the statistical analysis. N = 3 (B, D, and F), N = 4 (E), or N = 6 (C) individual experiments; each color (C and E) represents an independent experiment. Data are presented as mean ± SD (*$p \leq 0.05$; determined using one-way ANOVA together with Dunnett's post hoc test).

in antioxidant enzyme-overexpressing HEI-OC1 cells upon cisplatin treatment.

Together, these results indicated that ectopic expression of the selected human antioxidant enzymes could not protect HEI-OC1 cells from cisplatin-induced toxicity.

BCL-XL attenuates cisplatin-induced apoptosis of HEI-OC1 cells

Our previous results showed that treatment with cisplatin ultimately led to the death of HEI-OC1 cells (Figures 1 and S1), and we also detected signs of early apoptosis in cisplatin-treated HEI-OC1 cells (Figure 1E). Therefore, we hypothesized that the ectopic expression of genes that encode for the anti-apoptotic proteins BCL-2 and BCL-XL could protect HEI-OC1 cells from cell death during and after cisplatin treatment. Both anti-apoptotic proteins are localized at the outer mitochondrial membrane (OMM), where they inhibit the actions of the pro-apoptotic proteins BAK (BCL-2 antagonist/killer 1) and BAX (BCL-2 associated X).[59–62] These pro-apoptotic proteins initiate apoptosis by promoting permeabilization of the OMM and release of cytochrome c and ROS, which are important factors in the intrinsic apoptotic pathway.[63,64]

We generated SIN LV vectors expressing a codon-optimized version of human *BCL-2* (LV.BCL-2) or murine *Bcl-xl* (LV.BCL-XL), with 97% identity between the amino acid sequence of the human and murine version of the latter (Figure 3A).[65] HEI-OC1 cultures were transduced with the respective vector constructs and enriched for LV.BCL-2- or LV.BCL-XL-expressing cells via puromycin selection, followed by the confirmation of LV.BCL-2 or LV.BCL-XL protein expression by western blot analysis (Figure 3B). To assess the functionality of the proteins, we tested the influence of their ectopic

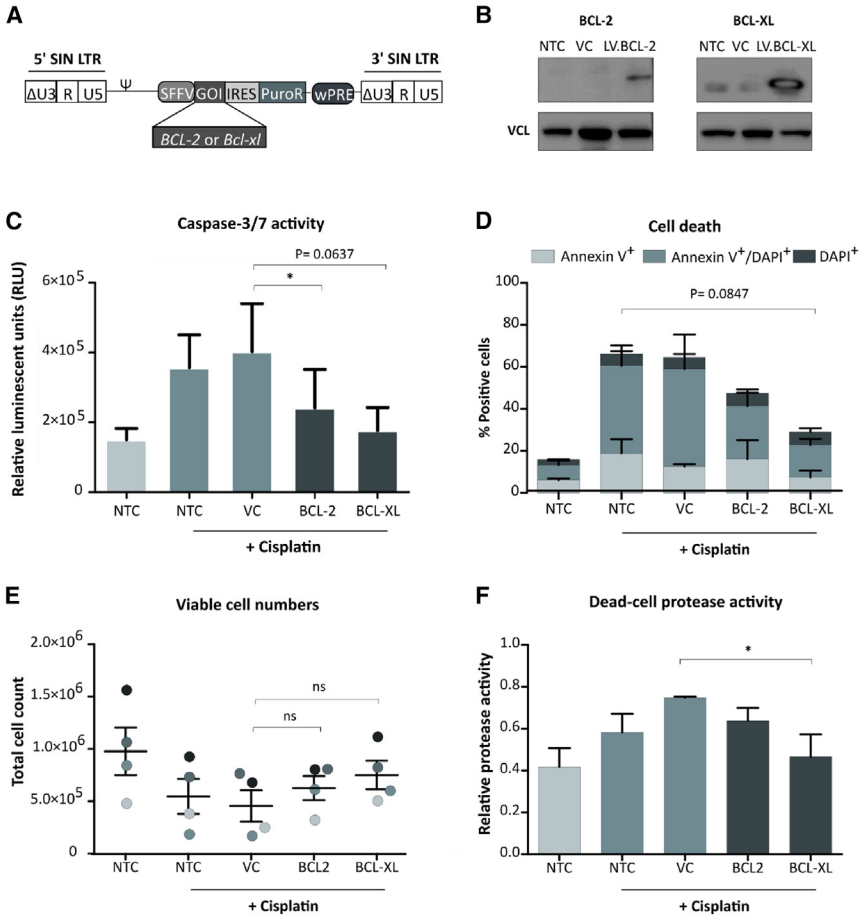

Figure 3. Ectopic expression of LV.BCL-2 and LV.BCL-XL protects HEI-OC1 cells from cisplatin-induced cytotoxicity

(A) Schematic overview of SIN LV vectors for the ectopic coexpression of human *BCL-2* or murine *Bcl-xl* with *PuroR*. (B) Representative western blot analysis of ectopically expressed BCL-2 (26 kDa) or BCL-XL (30 kDa) in transduced HEI-OC1 cells (LV) compared to NTCs and the VC. Endogenous VCL served as a loading control. (C) Caspase-3/-7 activity determined as RLUs in BCL-2 and BCL-XL-expressing, as well as HEI-OC1 control cells after treatment with cisplatin (5 μM, 72 h). (D) Percentage of early apoptotic (Annexin V^+) or dead ($DAPI^+$ or Annexin $V^+/DAPI^+$) cells from indicated HEI-OC1 cultures and conditions as determined by flow cytometry. (E) Total viable cell numbers in depicted untreated and cisplatin-treated (5 μM, 72 h) HEI-OC1 cultures. Each colored data point represents an individual experiment. (F) Cisplatin (5 μM, 72 h)-mediated relative dead-cell protease activity assessed using the ApoTox-Glo Triplex Assay. N = 3 (B–D and F) or N = 4 (E) individual experiments displayed as mean ± SD (*$p \leq 0.05$; determined using one-way ANOVA together with Dunnett's post hoc test).

overexpression on caspase-3/-7 activity and the percentage of Annexin V^+ cells upon cisplatin treatment because both are crucial markers indicating apoptotic cell death. LV.BCL-2 and LV.BCL-XL-overexpressing HEI-OC1 cells showed decreased caspase-3/-7 activity (Figure 3C) and reduced cell death rates as indicated by Annexin V^+/$DAPI^+$ cells (Figure 3D) compared to cisplatin-treated NTC or VC cultures. In direct comparison, LV.BCL-XL expression had a stronger effect than LV.BCL-2 expression and decreased the percentage of Annexin V^+ cells to a level comparable to that of untreated NTC. A reduction in apoptosis resulting from cisplatin treatment was also reflected in higher total cell counts (Figure 3E) and in decreased dead-cell protease activity upon LV.BCL-XL overexpression as compared to cisplatin-treated NTC and VC cultures (Figure 3F).

In summary, transgenic LV.BCL-XL was active and mediated anti-apoptotic effects that ultimately decreased the cytotoxicity of cisplatin treatment in HEI-OC1 cells.

Protective effect of BCL-XL in phoenix auditory neurons

In the *in vivo* cochlea, cisplatin exerts cytotoxic effects, especially in HCs and SGNs. Having shown that BCL-XL overexpression can rescue the HC-like HEI-OC1 cells from cisplatin toxicity, we next aimed at testing the capacity of our approach to also rescue SGN-like neurons. For this, we chose murine phoenix auditory cells derived from the A/J mouse cochlea as an *in vitro* culture system.[66]

The culture system was initially characterized in terms of self-renewal capacity, marker gene expression, neuroprogenitor sphere formation, and differentiation of spheres into auditory neurons, as described in the literature.[66,67] Phoenix spiral ganglion-derived neuroprogenitors formed spheres *in vitro* in the presence of defined growth factors (Figure 4A) and also showed self-renewing capacity (Figure S3A). Furthermore, the neuroprogenitor state was confirmed by the expression of the neural stem cells marker SOX2 (SRY-box transcription factor 2) and lack of expression of the mature neuronal marker MAP2 (microtubule-associated protein 2) and the glial cell marker GFAP (glial fibrillary acidic protein) (Figure 4B, left). Upon growth factor removal and cytokine addition, these auditory neuroprogenitors were successfully differentiated into bipolar phoenix auditory neurons, with successful differentiation demonstrated on day 6 by the lack of SOX2 expression in the presence of MAP2 and GFAP marker expression (Figure 4B, right).

To analyze whether phoenix neuroprogenitors and/or neurons can be used as a model to study cisplatin-induced toxicity, the cultures were exposed to cisplatin (5 and 20 μM, respectively) for 72 h. Untreated NTC phoenix auditory neuroprogenitors demonstrated sphere-forming capacity, whereas cisplatin-treated cells showed more dead cells, less sphere forming, and altered morphology of

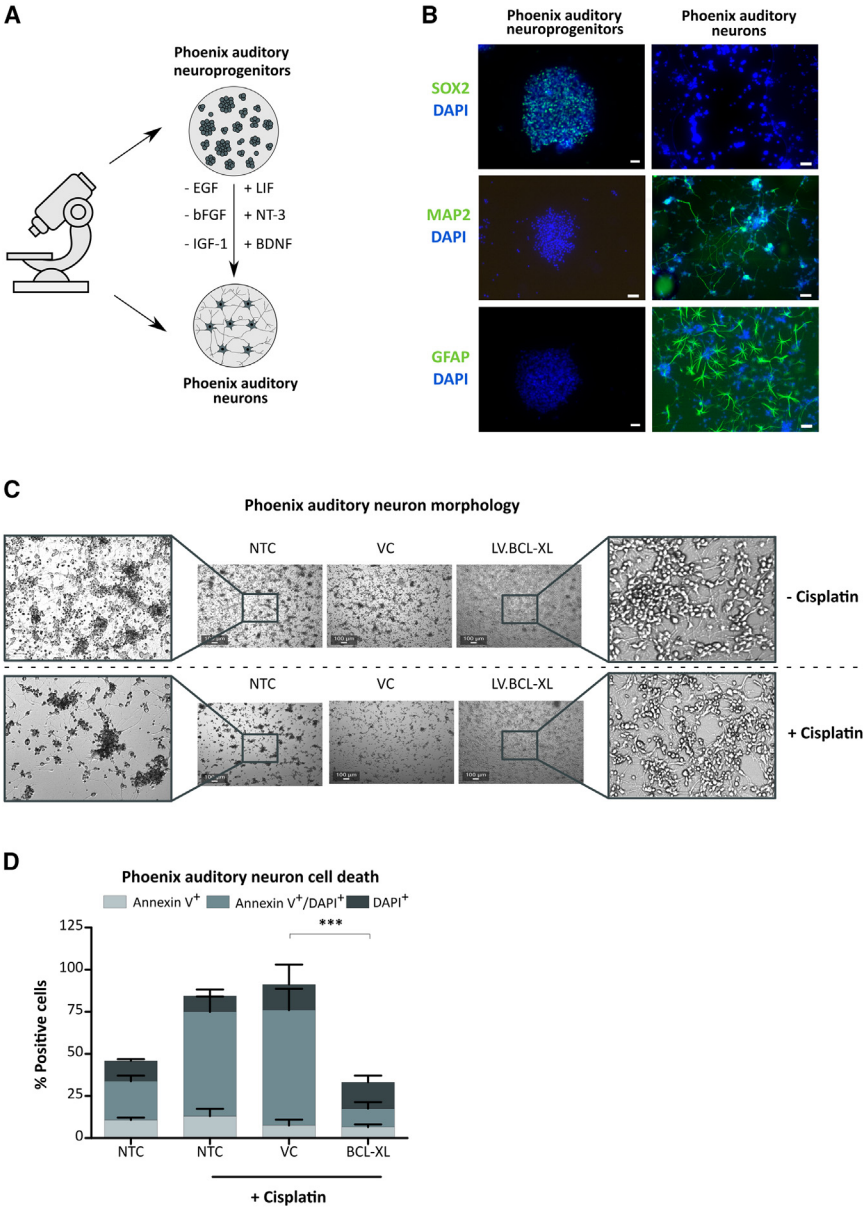

Figure 4. LV.BCL-XL rescues phoenix auditory neurons from cisplatin-induced cell death

(A) Schematic representation of the *in vitro* phoenix auditory neuroprogenitor and neuron differentiation model. The auditory neuroprogenitors grow as spheres in the presence of the growth factors EGF (epidermal growth factor), bFGF (basic fibroblast growth factor), and IGF-1 (insulin-like growth factor 1) and can be differentiated into auditory neurons by the withdrawal of EGF, FGF, and IGF-1 and the addition of the neurotrophic factors NT-3 (neurotrophin 3), BDNF (brain-derived neurotrophic factor), and the cytokine LIF (leukemia inhibitory factor). (B) Representative photographs of neuroprogenitors (left) and differentiated phoenix auditory neurons on day 6 of differentiation (right) analyzed by immunofluorescence analysis for the expression of neuronal markers. Both cell types were stained for the transcription factor and neural stem cell marker SOX2, the mature neuron marker MAP2, as well as the glial cell marker GFAP. Cell nuclei were stained with DAPI. Scale bar, 20 μm. (C) Live-cell images of differentiated NTCs, VC, and LV.BCL-XL phoenix auditory neurons on day 7 of differentiation, which had been cultivated for 72 h either in the presence (lower row) or absence (upper row) of 20 μM cisplatin. Scale bars, 100 μm. (D) Annexin V assay of cisplatin-treated (20 μM, 72 h) phoenix auditory neurons performed on day 6 of differentiation. The proportion of $DAPI^+$, Annexin V^+, and Annexin $V^+/DAPI^+$ cells are shown. N = 3 individual experiments. The data are depicted as mean ± SD (***$p \leq 0.001$; determined using one-way ANOVA together with Dunnett's post hoc test).

formed spheres (Figure S3A). Untreated phoenix auditory neurons showed the morphology of bipolar neurons in NTC cultures (Figure 4C), but upon cisplatin treatment, more dead cells were present in the medium, and the remaining adherent cells mainly showed soma and fewer cytoplasmic protrusions in the form of axons and dendrites.

To test whether this toxic effect of cisplatin could be prevented in phoenix auditory neuroprogenitors by the overexpression of the anti-apoptotic protein BCL-XL, the cells were transduced with LV.BCL-XL or the VC (Figure 3A) and subsequently selected for the expression of the transgene cassette by puromycin treatment. LV.BCL-XL expression was confirmed via western blot analysis (Figure S3B). The transduced phoenix auditory neuroprogenitors were then subjected to cisplatin treatment, followed by morphology and cell death analysis. Similarly to NTC phoenix auditory neuroprogenitors, cisplatin-treated VC cultures lost their sphere-forming ability and exhibited a higher number of dead single cells (Figure S3A). However, LV.BCL-XL phoenix auditory neuroprogenitors retained their sphere-forming capacity in various sizes and shapes following cisplatin treatment. The cell death experiments revealed high percentages of Annexin $V^+/DAPI^+$ cells in cisplatin-treated NTC (73.4%) (Figure S3C). Importantly, the overexpression of LV.BCL-XL kept the percentage of Annexin $V^+/DAPI^+$ cells (42.8%) at a level comparable to that of untreated NTC (40.8%).

LV.BCL-XL phoenix auditory neuron cultures contained more cells in general as well as more cells that displayed the bipolar neuron phenotype upon cisplatin treatment compared to NTC and VC cultures (Figure 4C). The Annexin V assay revealed increased percentages of dead cells (83.7%) after treatment with cisplatin in NTC phoenix auditory neurons (Figure 4D). Strikingly, ectopic expression of LV.BCL-XL led

to the complete protection of differentiated phoenix auditory neurons and showed even reduced levels of Annexin V^+/$DAPI^+$ cells (33.2%) when compared to untreated NTC cultures (46.9%).

To our knowledge, these results demonstrate for the first time that both phoenix neuroprogenitors and neurons represent a suitable model to study cisplatin-induced cytotoxicity. Furthermore, we showed that phoenix auditory neuroprogenitor cells could be stably transduced with SIN LV vectors. Finally, ectopic expression of the anti-apoptotic protein BCL-XL prevented cisplatin-induced cell death of both phoenix auditory neuroprogenitors and neurons.

BCL-XL decreases SGN death and maintains HC organization in rat cochlear explants upon cisplatin treatment

Because the results presented above demonstrated that ectopic expression of *Bcl-xl* counteracted cytotoxicity and significantly reduced the occurrence of dead and apoptotic cells in cisplatin-treated HEI-OC1, phoenix auditory neuroprogenitor, and differentiated phoenix auditory neuron cultures, we next examined the protective effect of the anti-apoptotic protein in primary SGNs and HCs (Figure 5).

To study the anti-ototoxic effect of the viral vector in primary SGNs, we used dissociated spiral ganglion cultures freshly prepared from neonatal rats (postnatal days 3–5 [P3–P5]). In addition to SGN, these cultures include fibroblasts and glial cells, which were discriminated by staining for expression of the surface markers CD90/Thy1 (cluster of differentiation 90/thymus antigen 1) and NGFR (nerve growth factor receptor) (Figure 5A).[68] While fibroblasts express only the surface protein CD90 ($CD90^+$), glial cells express only NGFR ($NGFR^+$) and type I SGNs (95% of the SGN culture) are considered double-negative for both surface markers ($CD90^-$ $NGFR^-$) at P3–P5.[69–71]

The spiral ganglion cell culture was transduced with LV.BCL-XL one day after organ extraction, and cisplatin was administered (20 μM, 48 h) 24 h post-transduction. Subsequently, cultures were analyzed by flow cytometry to detect the expression of NGFR and CD90 for cell discrimination and Annexin V/DAPI for cell death analysis. More $NGFR^+$ cells and, therefore, less SGN were detected in cisplatin-treated NTC, VC, and LV.BCL-XL cultures as compared to untreated NTC cultures (Figure 5B). Cell death analysis within the SGN population revealed increased percentages of Annexin V^+ and Annexin V^+/$DAPI^+$ SGN in cisplatin-treated NTC and VC cultures, whereas LV.BCL-XL-transduced cultures showed significantly reduced percentages of early apoptotic (Annexin V^+) cells, indicating a protective effect of LV.BCL-XL overexpression (Figure 5C).

To investigate the effect of LV.BCL-XL overexpression in primary HCs upon cisplatin treatment, rat cochlear explants (P3–P5) were transduced with LV.BCL-XL and subsequently treated with cisplatin as before (50 μM, 48 h). For analysis, the explants were stained for MYO7A (myosin VIIA) expression to specifically identify HCs (Figure 5D). While the typical three rows of OHC and one row of inner HCs (IHCs) were detected in untreated explants, HC organization was destroyed in cisplatin-treated NTC or VC explants, and HC death was observed as individual HCs were missing, visible as gaps in the HC rows. In contrast, better maintenance of HC organization and increased HC survival were observed in explants transduced with LV.BCL-XL.

Together, these results confirmed that overexpression of the anti-apoptotic protein BCL-XL protected primary otic cells from cisplatin treatment.

BCL-XL overexpression protects cisplatin-treated mice from high-frequency hearing loss and OHC death

Overexpression of the anti-apoptotic gene *Bcl-xl* prevented cisplatin toxicity in several *in vitro* and *ex vivo* model culture systems (Figures 3, 4, and 5). Therefore, we next evaluated the effect of LV.BCL-XL *in vivo* in a cisplatin challenge experiment using normal-hearing C57BL/6 mice.

ABR measurements at P35 and before LV.BCL-XL gene therapy confirmed normal hearing of the mice at different frequencies between 4,000 and 32,000 Hz, thus covering the entire hearing range (Figures 6A and S4A). LV.BCL-XL was then administered via canalostomy into one ear of each mouse (LV.BCL-XL gene therapy). Five days after vector injection, ABR measurement was repeated and demonstrated normal thresholds, thus excluding any negative effect of vector administration and LV.BCL-XL expression on hearing capacity. Subsequently, 4 mg/kg cisplatin were administered intraperitoneally by daily injection over 5 consecutive days, reflecting standard treatment regimen protocols for cancer patients.[72] At P47 and P57 after the last cisplatin dose, ABR measurements were performed for gene therapy-treated ears as compared to the NTC contralateral control ears to determine the effects of cisplatin and LV.BCL-XL treatment.

Cisplatin treatment resulted in higher ABR thresholds in ears that had not received LV.BCL-XL vector particles (no gene therapy), implying hearing loss (Figures 6B and S4B). Although mild hearing loss was also observed at the low frequencies, higher effects were detected with ABR thresholds >40 dB at the high frequency range ($\geq$16,000 Hz). Notably, in LV.BCL-XL gene therapy ears, cisplatin-mediated hearing loss was strongly diminished, with only minor hearing restrictions after cisplatin treatment. In line with this, histochemical staining of the cochlear base, which processes high sound frequencies, revealed intact IHC and OHC rows without gaps in LV.BCL-XL gene therapy ears, whereas OHCs but not IHCs were damaged in the no-gene therapy contralateral control cochleae (Figures 6C, 6D, and S5A). The graph in Figure 6D summarizes the results from four mice and confirmed that LV.BCL-XL expression preserved the abundance of OHC in the cochlear base upon cisplatin treatment, with significantly higher OHC counts per 50-μm section in the LV.BCL-XL gene therapy as compared to the no-gene therapy control ears. In addition, the HC counts from LV.BCL-XL-injected ears of mice treated with cisplatin are similar to those from mice injected with LV.BCL-XL without cisplatin treatment (Figure S5C). Interestingly, in the apex of the cochlea, which is responsible for

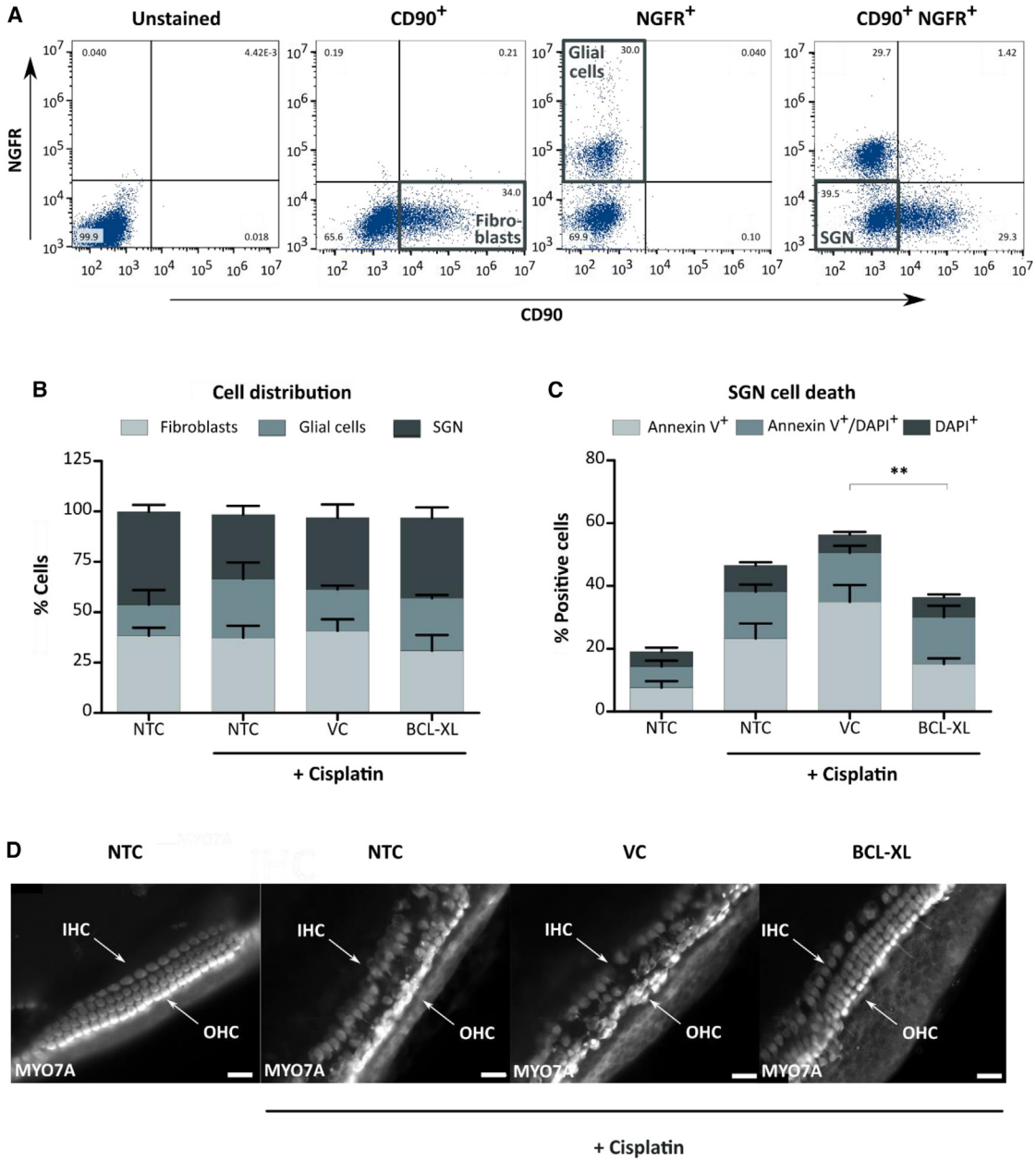

Figure 5. Ectopic expression of LV.BCL-XL prevents the death of primary SGNs and HCs upon cisplatin treatment

(A) Representative flow cytometry plots showing CD90 and NGFR staining of spiral ganglion cell cultures to distinguish fibroblasts ($CD90^+$ $NGFR^-$), glial cells ($CD90^-$ $NGFR^+$) and SGNs ($CD90^-$ $NGFR^-$). (B) Proportion of fibroblasts, glial cells, and SGNs among spiral ganglion cultures after 48 h treatment with 20 μM cisplatin or untreated control. (C) Percentage of Annexin V^+, $DAPI^+$, and Annexin V^+/$DAPI^+$ cells as determined by flow cytometry to assess the cell death of spiral ganglion cultures after cisplatin treatment (20 μM, 48 h) as compared to non-treated controls. (D) Representative pictures of NTCs and LV.BCL-XL engineered cochlea explants stained for MYO7A after treatment with 50 μM cisplatin for 48 h. HCs were identified based on MYO7A expression and were arranged in one row of IHCs and three rows of OHCs. Scale bar, 20 μm. N = 3 (A–D). The data in the bar graphs are depicted as mean ± SD (**$p \leq 0.01$; determined using one-way ANOVA together with Dunnett's post hoc test).

the processing of low sound frequencies, OHCs and IHCs were not affected by cisplatin treatment, explaining why no significant differences in the ABR measurement were detected upon cisplatin treatment as compared to the pre-cisplatin thresholds at frequencies of 4,000 and 8,000 Hz (Figure 6B). As a marker for early apoptosis, Annexin V staining indicated that the affected cells within the organ of Corti, presumably the OHCs, underwent apoptosis in the cochlea without gene therapy (Figure S5B).[52] However, fewer early apoptotic

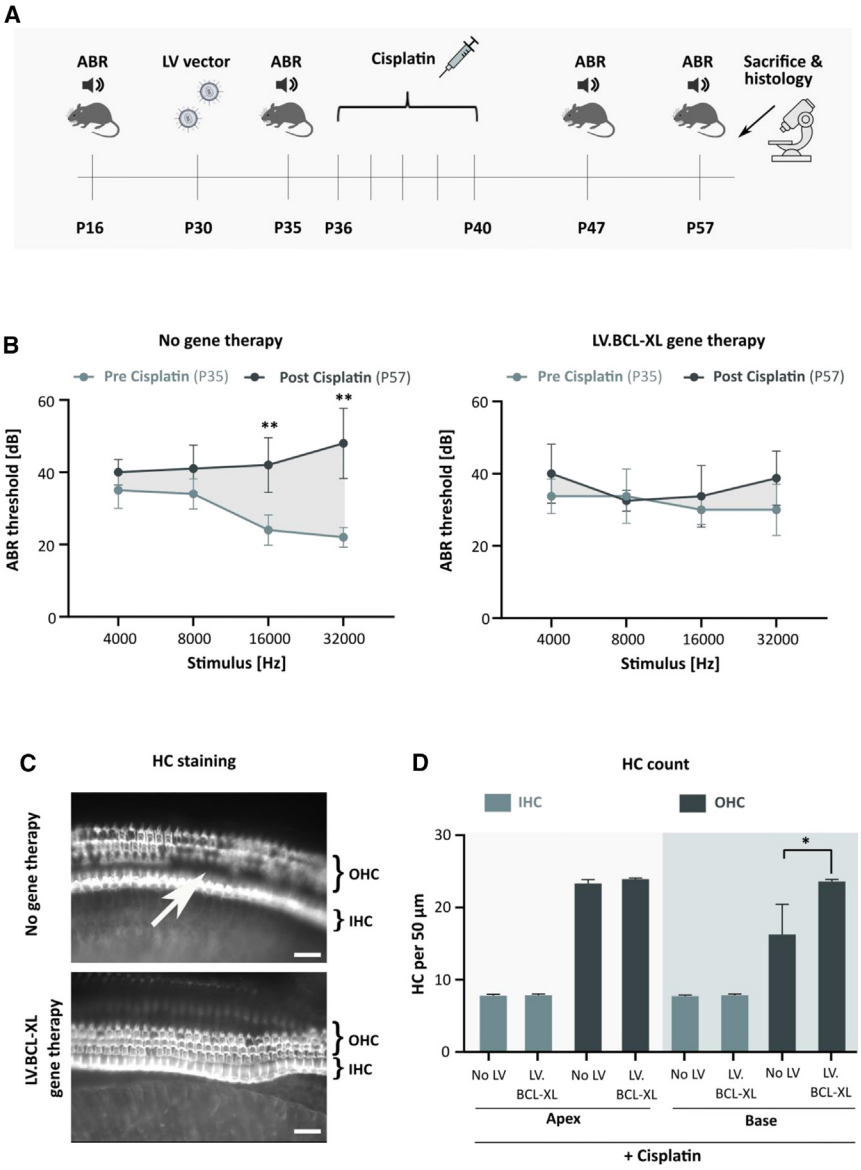

Figure 6. LV.BCL-XL gene therapy rescues OHCs and impedes high-frequency hearing loss in cisplatin-treated C57BL/6 mice

(A) Schematic overview of the *in vivo* experiment. ABR measurement was performed before gene therapy (P16), followed by canalostomy and injection of LV.BCL-XL particles into one ear of each mouse (P30). ABR measurement was repeated before cisplatin treatment (P35), followed by daily cisplatin administration on P36–P40, and final ABR measurements on P47 and P57, as well as histological analyses at end analysis. (B) ABR thresholds before (P35) and after (P57) cisplatin treatment in control ears without LV.BCL-XL injection (no gene therapy, left) and ears injected with LV.BCL-XL (right). N = 4 mice. (C) Representative photographs of phalloidin-stained, basal turns of the cochlea collected at end analysis after cisplatin treatment to compare effects in ears that did not receive gene therapy with those treated with LV.BCL-XL. Arrow: area with large gaps in one OHC row in the non-treated cochlea. Scale bar, 50 µm. (D) HC counts in the base and apex of cochleae from ears with or without LV.BCL-XL gene therapy, obtained from cisplatin-treated mice at end analysis. N = 4 mice. The data are depicted as mean ± SD (*$p \leq 0.05$, **$p \leq 0.01$; determined using one-way ANOVA and Dunnett's post hoc test).

cells were observed in the LV.BCL-XL cochlea, implying that the anti-apoptotic protein BCL-XL also prevented apoptosis of inner ear cells such as OHCs *in vivo*.

In conclusion, canalostomy injection of LV.BCL-XL prevented OHC death in the cochlear base and thus suppressed high-frequency hearing loss in cisplatin-treated mice.

DISCUSSION

Cisplatin is a very effective chemotherapeutic agent, but its administration is associated with severe side effects, including ototoxicity.[73–76] Since international regulatory agencies have so far only approved a single prevention or treatment regimen against cisplatin-induced ototoxicity in the United States, patients receiving cisplatin must still be monitored closely and the dose must be reduced to minimize adverse effects.[77] However, this also decreases its anti-tumor activity.[78] To circumvent this conflict, our study aimed to develop a gene therapy strategy to prevent cisplatin-induced hearing loss.

To design a gene therapy option, we considered and addressed known facts and published data on the mechanism of cisplatin-induced ototoxicity. Cisplatin leads to the increased production of ROS in OHCs and SGNs, which eventually leads to cell damage and induction of PCD in the affected cells.[20–22,48,50] Therefore, our approach was to specifically intervene in these cellular pathways and to either reduce the elevated ROS levels by ectopic expression of the antioxidant enzymes SOD1, CAT, or GPX1, or prevent PCD by apoptosis via the overexpression of the anti-apoptotic proteins BCL-2 or BCL-XL.

In vitro testing of these proteins in HEI-OC1 cells revealed that only the anti-apoptotic proteins BCL-2 and BCL-XL were protective in terms of rescue from cisplatin-induced cytotoxicity. In phoenix auditory neurons as well as primary SGNs and HCs, LV.BCL-XL was functional and protected the cells from cisplatin toxicity. Strikingly, *in vivo*, LV.BCL-XL overexpression prevented the loss of OHCs in the base of the cochlea, which abrogated high-frequency hearing loss in cisplatin-treated mice after cisplatin treatment until

the end of the study (21 days). This is the first report demonstrating that BCL-XL can prevent hearing loss after cisplatin treatment in mice.

Although an early intervention in the toxicity pathway of cisplatin is considered advantageous, our results revealed that preventing apoptosis was more effective than reducing oxidative stress by the ectopic overexpression of SOD1, CAT, or GPX1. Even though we could show the activity of lentivirally expressed antioxidant enzymes in HEI-OC1 cells (Figures 2C and 2D), LV.SOD1, LV.CAT, and LV.GPX1 were unable to significantly reduce cisplatin-induced toxicity *in vitro* (Figure 2F). The concept of specifically testing SOD1 and GPX1 in our study was based on the fact that these two isoforms are the most abundant antioxidant enzymes in the cochlea.[54,55] However, several other isoforms of the antioxidant enzymes SOD and GPX are also expressed and differ in their localization and cofactors.[57,79] Since SOD is responsible for catalyzing the first reaction in the process of detoxifying superoxide anions, this antioxidant enzyme family was selected in several studies, with a focus on SOD2, which is located within mitochondria. One study tested the ectopic expression of SOD1, SOD2, and CAT via adenoviral vectors in kanamycin-treated mice.[80] Here, CAT and SOD2 showed beneficial effects in protection from HC loss and hearing loss, whereas the results obtained with SOD1 were inconsistent. However, Ohlemiller *et al.* demonstrated that SOD1 plays an important role in preventing noise-induced hearing loss (NIHL), since SOD1 knockout mice showed increased susceptibility to NIHL.[81] In contrast, the knockdown of SOD2 in cisplatin-treated HEI-OC1 cells had only a minor effect on cytotoxicity.[82] Hence, these published data and the results from our study highlight that the strategy to reduce ROS via antioxidant enzymes to protect patients from drug-induced hearing loss provides inconsistent results, and the success of these strategies may depend on the hearing loss-inducing agent or stimulus whose toxic effects are intended to be counteracted.

Similar to our study, the ectopic expression of anti-apoptotic proteins in cisplatin-induced hearing loss models has shown beneficial effects in previous studies. Cooper *et al.* showed that round window injection of an adeno-associated virus (AAV) vector expressing the caspase inhibitor X-linked inhibitor of apoptosis protein could prevent an increase in ABR thresholds and loss of OHCs.[83] Furthermore, another study reported that BCL-2 delivered into cells by an adenoviral vector resulted in increased HC and SGN survival in rats after cisplatin treatment.[84] In our hands, BCL-XL provided stronger and more robust *in vitro* results than BCL-2. Therefore, it is a highly interesting candidate for further investigation to develop a prevention strategy against cisplatin-induced hearing loss.

Although all of the previous reports were based on AAV or adenoviral vectors for transgene delivery and expression, we used an LV SIN vector platform. The vectors expressed PuroR, which allowed the selection of transduced cells *in vitro*, including phoenix cells. However, selection was not an option for primary SGNs and HCs because these were integrated into the multidimensional tissue of cochlea explants, nor could selection be applied *in vivo*. Accordingly, no conclusions can be derived as to which cells were transduced or what percentage of target cells were transduced. Nevertheless, detailed characterization of LV inner ear transduction in other contexts has demonstrated their general capability to efficiently transduce multiple cells types within the cochlea, including HCs and SGNs, and—importantly—a protective effect was observed in the present study in primary material as well as *in vivo* upon LV.BCL-XL application, indirectly confirming successful transduction.[85] However, the inclusion of a fluorescent reporter on the vector in future studies would be helpful to address transduction efficiency and to more closely delineate the type of transduced cells. In our study, we observed that the expression of one of the most commonly used fluorescent reporters, EGFP, in cisplatin-treated HEI-OC1 cells alone had a beneficial effect because it reduced cytotoxicity (Figure S2B), thus precluding its use in settings addressing cisplatin toxicity. The observed effect is presumably due to the requirement of molecular oxygen for chromophore formation/maturation and the associated oxygen-scavenging property of this and other fluorescent proteins.[86] Since cisplatin increases the production of ROS, caution must be taken when performing cytotoxicity analyses in EGFP-expressing cells, and therefore, alternatives to EGFP will be needed, such as eUnaG, a fluorescent protein from Japanese eel. Because the formation and maturation of eUnaG is independent of oxygen, this fluorescent protein could be coexpressed with the effector gene to study cisplatin-induced ototoxicity in the future.[87]

Furthermore, despite several advantageous characteristics of SIN LV vectors over other vector platforms, including low immunogenicity, the option to generate high titers through concentration, and a high-coding-capacity, constitutive expression of an anti-apoptotic gene to prevent toxic side effects of cisplatin as mediated by this integrating vector family will likely not be applicable in clinical settings.[39,40] Therefore, one possibility to optimize this gene-therapeutic approach is to implement regulated gene expression. This would allow BCL-XL expression to be switched on for each round of cisplatin chemotherapy and to be shut off again thereafter. For example, regulated gene expression could be achieved by an antibiotic-inducible and, therefore, controlled expression of the transgene (e.g., using tetracycline-based systems) or by targeted proteasomal degradation of the transgene (e.g., using the destabilizing domain of *Escherichia coli* dihydrofolate reductase).[88–93]

In addition to a regulated gene expression, the SIN LV vector could be optimized to increase safety and restrict the expression of the transgene to the cells most affected by cisplatin treatment. This could be achieved by the incorporation of a cell-type-specific promoter that would allow expression specifically in HCs or SGNs. For HCs, the Myo7A promoter is conceivable, whereas the synapsin 1 or MAP1B promoter could drive expression in SGNs.[94–96] Lastly, the tropism of the LV vector could be restricted to the target cells by pseudotyping with specific glycoproteins.[38]

In summary, we present a gene therapy approach using SIN LV vectors to ectopically express the anti-apoptotic protein BCL-XL, which prevented cisplatin-induced hearing loss *in vivo* in mice. Since the approach to reduce the oxidative stress in affected cells showed no effect *in vitro*, research focused on prevention of PCD in OHCs and SGNs could be effective and beneficial in the future.

MATERIALS AND METHODS

Cell culture

HEK293T cells (ACC 635, DSMZ, Braunschweig, Germany) were cultured at 37°C and 5% CO_2 in high-glucose DMEM (Gibco/Thermo Fisher Scientific, Schwerte, Germany) with 10% heat-inactivated fetal bovine serum (FBS), 100 U/mL penicillin, 100 μg/mL streptomycin, and 1 mM sodium pyruvate (all from PAN Biotech, Aidenbach, Germany). The murine auditory cell line HEI-OC1, kindly provided by Federico Kalinec (House Ear Institute, Los Angeles, CA, USA), was cultured at 33°C and 10% CO_2 in high-glucose DMEM containing 10% heat-inactivated FBS, 100 U/mL penicillin, and 1 mM sodium pyruvate.[42] HEI-OC1 cells stably expressing a puromycin resistance gene were cultured in the above medium additionally supplemented with 6 μg/mL puromycin (InvivoGen, Toulouse, France). Phoenix auditory neuroprogenitors were kindly provided by Francis Rousset and Pascal Senn (University of Geneva, Geneva, Switzerland) and cultured in ultra-low attachment plates (Corning/Sigma-Aldrich, Munich, Germany) in proliferation medium consisting of DMEM/F12 (Gibco/Thermo Fisher Scientific), 15 mM HEPES (Pan Biotech), 1× N_2 and B27 supplement (both Gibco/Thermo Fisher Scientific), 100 U/mL penicillin, 50 ng/mL heparan sulfate (kindly provided by Falk Büttner, Hannover Medical School, Hannover, Germany), 50 ng/mL human insulin-like growth factor 1 (IGF-1), 10 ng/mL human basic fibroblast growth factor (bFGF), and 20 ng/mL human epidermal growth factor (EGF) (all Peprotech, Hamburg, Germany).[66,67] Phoenix auditory neuroprogenitor cultures stably expressing a *PuroR* gene were selected with 0.3 μg/mL puromycin before analyses. For differentiation into phoenix auditory neurons, the phoenix cells were cultivated in DMEM/F12 with 15 mM HEPES, 1× N_2 and B27 supplement, 100 U/mL penicillin, 10 ng/mL human leukemia inhibitory factor (LIF), 50 ng/mL human neurotrophin 3 (NT-3) and 10 ng/mL human/mouse/rat brain-derived neurotrophic factor (BDNF) (all Peprotech; differentiation medium) on Geltrex-coated (Gibco/Thermo Fisher Scientific) cell culture plates.

Preparation and culture of neonatal rat primary SGNs and cochlea explants

Primary spiral ganglion cells were isolated from neonatal Sprague-Dawley rats on P3–P5 in accordance with the German Animal Welfare Act. The euthanasia is registered (no. 2016/118) with the local authorities (Zentrales Tierlaboratorium, Laboratory Animal Science, Hannover Medical School, including an institutional animal care and use committee) and is reported on a regular basis as demanded by law. For exclusive sacrifice of animals for tissue analysis in research, no further approval is needed if no other treatment is applied beforehand (§4). The preparation of the spiral ganglion and the subsequent enzymatic and mechanic dissociation was performed as described elsewhere.[97] The obtained spiral ganglion culture constitutes a mixture of SGNs, fibroblasts, and glial cells seeded on poly-D/L-ornithine- (0.1 mg/mL; Sigma-Aldrich) and laminin (0.01 mg/mL; Life Technologies, Carlsbad, CA)-coated 48-well plates. This spiral ganglion cell culture was cultivated in serum-free Panserin 401 medium (PAN Biotech) supplemented with 25 mM HEPES (Life Technologies), 6 mg/mL glucose (Braun AG, Melsungen, Germany), 30 U/mL penicillin (Grünenthal GmbH, Aachen, Germany), 3 μg/mL N_2 supplement (Life Technologies), and 5 μg/mL insulin (Sigma-Aldrich) at 37°C and 5% CO_2. Cochlear epithelia were collected from neonatal Sprague-Dawley rats at P3–P5 as previously described.[98] The prepared cochlear explants were cultivated on Nucleopore Track Etch membranes (Whatman, Maidstone, UK) floating on medium containing DMEM/F12 (PAN Biotech), 1:1 MACS NeuroBrew21 (Miltenyi, Bergisch Gladbach, Germany), 1 mM N-acetylcysteine (Sigma-Aldrich), 5 ng/mL EGF (Gibco), 2.5 ng/mL bFGF (Gibco), and 100 U/mL penicillin (Sigma-Aldrich) in 4-well plates (Thermo Fisher Scientific).

Experimental animals

C57BL/6 mice were purchased from The Jackson Laboratory (Bar Harbor, ME, USA) and maintained in a breeding colony. The Institutional Animal Care and Use Committee (IACUC) from the University of Kansas approved all of the animal care and procedures under IACUC protocol 2018–2442.

Cloning of LV vector plasmids

The SIN LV vector plasmid pRRL.PPT.SFFV.GOI.IRES.PuroR.PRE served as the backbone for the constructs used in this manuscript. The promoter of the spleen focus forming virus (SFFV) drives expression of the respective gene of interest (GOI), which is followed by an internal ribosomal entry site (IRES) to initiate *PuroR* gene expression. The GOI *SOD1*, *CAT*, *GPX1*, *BCL2*, and *Bcl-xl* were inserted into the LV vector backbone via AgeI and SalI restriction sites.

Production of LV vector particles

SIN LV vector particles were produced as previously described by transient calcium-phosphate transfection of HEK293T cells.[99] Briefly, the day before transfection, 5×10^6 HEK293T cells were seeded per 10-cm culture dish. For the generation of vesicular stomatitis virus envelope glycoprotein G (VSVg)-pseudotyped SIN LV vector particles, 5 μg of the respective SIN LV vector plasmid were cotransfected with 12 μg LV wild-type Gag-Pol (pcDNA3.wtHIV-1.G/P.4xCTE),[99] 5 μg Rev (pRSV.Rev, kindly provided by Thomas J. Hope, Northwestern University, Chicago, IL), and 2 μg VSVg (pMD.G)[100] expression plasmid. Transfection was performed in the presence of 20 mM HEPES and 25 μM chloroquine (Sigma-Aldrich). SIN LV vector particle-containing supernatants were harvested at 24 and 48 h post-transfection, filtered (0.22 μm), pooled, and subsequently concentrated 100-fold by ultracentrifugation for 2 h at 82,740 × *g* and 4°C.

Transduction of target cells with SIN LV vector particles and *in vivo* delivery

The day before transduction, 5×10^4 HEI-OC1 cells were seeded per well of a 12-well plate. For the transduction of phoenix auditory neuroprogenitors, 1×10^5 cells were seeded per well of a 24-well ultra-low attachment plate directly before transduction. Transduction was performed at an MOI (multiplicity of infection) of 1, in a volume of 500 μL, and in the presence of 4 μg/mL protamine sulfate (Sigma-Aldrich). In the case of HEI-OC1 cells, transduction was supported by centrifugation for 1 h at 800 × *g* and 33°C.

For the transduction of primary spiral ganglion cells, 1×10^4 cells were seeded per well in 48-well plates the day before transduction. The amount of SIN LV vector particles was adapted to 1×10^6 particles for transduction in 100 μL culture medium containing 4 μg/mL protamine sulfate. Subsequently, the plate was centrifuged for 1 h at 800 × *g* and 37°C.

Primary cochleae were prepared and cultured on Nucleopore track-etched membranes for one day before transduction. For the transduction, the concentration of the LV vector was adjusted to 5×10^6 particles in 50 μL protamine sulfate (4 μg/mL)-containing culture medium and was administered directly onto the cochleae. After incubation for 30 min at 37°C and 5% CO_2, 300 μL of the culture medium containing 4 μg/mL protamine sulfate was added.

C57BL/6 mice (1 month old) were intraperitoneally injected with ketamine (150 mg/kg), xylazine (6 mg/kg), and acepromazine (2 mg/kg) in 0.9% sodium chloride for anesthesia, followed by a dorsal postauricular incision to disclose the posterior semicircular canal. To expose the perilymphatic space, a microdrill was used, and subsequently, with the help of a Hamilton microsyringe with 0.1 μL graduations and a 36G needle, 1 μL of the LV.BCL-XL vector was injected into the defined perilymphatic space. The injection site was closed with bone wax, and the C57BL/6 mice recovered from this procedure for 5 days before their hearing was analyzed via ABR.

Analysis of antioxidant enzyme activity

To determine SOD activity in cisplatin-treated and nontreated cells, 5×10^5 NTC and LV.SOD1-overexpressing HEI-OC1 (SOD1-HEI-OC1) cells were seeded. The next day, NTC and SOD1-HEI-OC1 cultures were incubated in the absence or presence of 5 μM cisplatin for 72 h. Finally, SOD activity was measured by the Superoxide Dismutase Activity Assay Kit (Colorimetric) (Abcam, Cambridge, UK) following the manufacturer's instructions. To measure CAT or GPX enzyme activity, 5×10^4 NTC and antioxidant enzyme-overexpressing HEI-OC1 cells were treated with 500 μM H_2O_2 for 48 h. Subsequently, H_2O_2-mediated cytotoxicity was assessed via allophycocyanin (APC)-Annexin V/DAPI staining and flow cytometry by using the CytoFLEX S.

Cytotoxicity assays

To determine cell viability and cytotoxicity after cisplatin treatment in HEI-OC1 cells, different assays were performed, in which the cellular and metabolic changes were measured that are associated with viable or dead cells. Therefore, 5×10^4 or 2×10^3 cells were seeded in 12- or 96-well Nunc MicroWell plates (Thermo Fisher Scientific), respectively. The following day, the cells were treated with 5 μM cisplatin for 72 h. Subsequently, cells seeded in the 96-well plates were analyzed for dead-cell protease activity and caspase-3/-7 activity using the ApoTox-Glo Triplex Assay Kit (Promega, Walldorf, Germany) following the manufacturer's instructions. The degree of cell destruction within the treated cultures was investigated with the help of a cell-impermeant fluorogenic peptide substrate, which can be cleaved only by cellular proteases released upon cell death. The "dead-cell protease activity" is expressed as relative fluorescent units (RFUs) and reflects the amount of proteolytically cleaved fluorogenic substrate within the culture medium. In contrast, caspase-3/-7 activity was assessed after cell lysis by adding a luminogenic caspase-3/-7 substrate to the lysates. The latter is cleaved by caspase-3 and -7, thereby generating luciferin, which is converted into oxyluciferin and visible light by a recombinant luciferase. Thus, caspase-3/-7 activity is indirectly determined by a luciferase reaction and measured in relative luminescent units (RLUs). The readout of the assay was performed using either the SpectraMax Paradigm Multi-Mode Microplate Reader (Molecular Devices, Munich, Germany) or the GloMax Explorer Multi-Mode Microplate Reader (Promega).

Cells seeded in the 12-well plates were used either to determine the cell numbers or to analyze the induction of cell death. The adherent cells were harvested for cell count analysis, and cell numbers were determined by analyzing 60 μL of each sample with the CytoFLEX S (Beckman Coulter, Indianapolis, IN, USA) flow cytometer and subsequent calculation of the total cell number per well. The induction of cell death was assessed by harvesting the adherent cells as well as dead cells from the medium and subsequent staining with APC-Annexin V (1:200, BD Biosciences, Heidelberg, Germany, catalog no. 550474) for 10 min at room temperature in the dark. This was followed by staining with 0.2 μg/mL DAPI (Sigma-Aldrich). The cells were immediately analyzed by flow cytometry using the CytoFLEX S.

To study the cytotoxic effect of cisplatin in phoenix auditory neuroprogenitors and phoenix auditory neurons, treated cells were stained and analyzed with APC-Annexin V and DAPI and analyzed via flow cytometry, as described above. Phoenix auditory neuroprogenitors were seeded in a density of 1×10^5 cells in 24-well ultra-low attachment plates in proliferation medium and treated with 5 μM cisplatin for 72 h. A total of 5×10^4 phoenix auditory neuroprogenitor cells were seeded onto Geltrex-coated 24-well plates in differentiation medium for differentiation into phoenix auditory neurons. On day 4 of differentiation, fresh differentiation medium was added, and 20 μM cisplatin was administered for 72 h. The Annexin V assay was performed on day 7 of differentiation.

The primary spiral ganglion culture was treated for 48 h with 20 μM cisplatin the day after transduction. Subsequently, co-staining was performed with Alexa Fluor 647-CD90.1 (1:200, BioLegend, Koblenz,

Germany, catalog no. 100750) and fluorescein isothiocyanate (FITC)-NGFR (1:100, Santa Cruz Biotechnology, Heidelberg, Germany, catalog no. sc-71691) for 20 min at 4°C in the dark. This staining was followed by phycoerythrin-Annexin V (1:200, BD Biosciences, catalog no. 556422) and DAPI staining and subsequent flow cytometry analysis, as described previously.

Determination of ROS production

The production of ROS was analyzed with the cell-permeable and nonfluorescent H_2DCFDA (2′,7′-dichlorodihydrofluorescein diacetate; Thermo Fisher Scientific) following the manufacturer's instructions. The percentage of DCF^+ cells was analyzed using the CytoFLEX S flow cytometer.

Immunofluorescence

Phoenix auditory neuroprogenitors, differentiated phoenix auditory neurons, or cochleae were fixed in 4% paraformaldehyde for 15 min at room temperature and rinsed with PBS. Fixed samples were permeabilized in 0.2% Triton X-100 in PBS for 10 min at room temperature and subsequently blocked with 5% FBS in PBS for 30 min. The samples were incubated with the primary antibodies rabbit-anti-MYO7A (1:100, Proteus Biosciences, Ramona, CA, catalog no. 25–6790), mouse-anti-NF200 (1:200, Leica Biosystems, Wetzlar, Germany, catalog no. NF200-N52-L-CE), rabbit-anti-SOX2 (1:500, Abcam, catalog no. AB97959), rabbit-anti-MAP2 (1:500, Sigma-Aldrich, catalog no. AB5622), or mouse-anti-GFAP (1:100, Sigma-Aldrich, catalog no. MAB360) in PBS overnight at 4°C in PBS supplemented with 0.5% BSA and 0.1% Triton X-100. The samples were washed three times with 0.1% Triton X-100 in PBS and incubated with the secondary antibodies donkey-anti-rabbit conjugated with Alexa Fluor 488 (1:500, Jackson Immuno Research, Ely, UK, catalog no. 711-545-152) or goat-anti-mouse conjugated with Alexa Fluor 555 (1:500, BioLegend, catalog no. 405324), respectively, for 1 h at room temperature. Prestained phoenix auditory neuroprogenitors and neurons were counterstained with 1 μg/mL DAPI in PBS immediately before mounting in Invitrogen ProLong Gold Antifade Mountant (Thermo Fisher Scientific). Finally, the samples were inspected under a phase contrast fluorescence Zeiss Axio Observer Z1 microscope (Zeiss, Oberkochen, Germany).

Live-cell imaging

The morphology of phoenix auditory neuroprogenitors and neurons was monitored over time using the live-cell imaging device Cellcyte X (Cytena, Freiburg, Germany). To achieve this, 5×10^4 phoenix neuroprogenitor cells were seeded in 24-well plates (Corning/Sigma-Aldrich) in the appropriate medium for either proliferation or differentiation. Following seeding, the phoenix auditory neuroprogenitors were exposed to cisplatin, after which the analysis of sphere formation and morphology commenced. The cells used for differentiation into phoenix auditory neurons underwent cisplatin treatment on day 4 of differentiation. Following this, live-cell imaging was initiated in an incubator set at 37°C and 5% CO_2. Each condition was measured in triplicate, and each well was imaged with a 4× objective once every 2 h over a period of 3 days in the enhanced contour (bright-field analog) channel.

Total protein extraction and western blot analysis

HEI-OC1 or phoenix neuroprogenitor cells were lysed to detect transgene expression with a buffer containing 50 mM HEPES, 150 mM NaCl, 50 mM NaF, 10 mM $Na_4P_2O_7$, 10% glycerin, and 1% Triton X-100. A total of 30 μg of each total protein sample were separated by an SDS-PAGE and transferred to a nitrocellulose membrane (GE Healthcare Life Science, Solingen, Germany). The membrane was blocked with 3% milk powder (Roth, Karlsruhe, Germany) dissolved in Tris buffered saline-Tween-20 (TBST) buffer for 1 h at room temperature and probed overnight at 4°C with either anti-SOD1 (1:1,000, Thermo Fisher Scientific, catalog no. MA5-15520), anti-CAT (1:1,000, Origene, Herford, Germany, catalog no. TA502564) anti-GPX1 (1:1,000, Thermo Fisher Scientific, catalog no. MA5-32848), anti-BCL2 (1:1,000, Cell Signaling Technology, catalog no. 3498) or anti-BCL-XL (1:1,000, Cell Signaling Technology, catalog no. 2764) in 3% milk powder in TBST buffer. As secondary antibodies, goat-anti-rabbit immunoglobulin G (IgG) (1:4,000, Cayman Chemical Company, Ann Arbor, MI, catalog no. 10004301) or goat-anti-mouse IgG (1:4,000, Cayman Chemical Company, catalog no. 10004302) conjugated with horseradish peroxidase (HRP) were used. Protein bands were detected with the SuperSignal West Pico Chemiluminescent Substrate (Thermo Fisher Scientific) and quantified using the FUSION FX imaging system (Vilber Lourmat, Eberhardzell, Germany). Equal protein loading was demonstrated by staining the membrane with an HRP-conjugated anti-glyceraldehyde 3-phosphate dehydrogenase antibody (GAPDH; 1:10,000, Biozol, Eching, Germany, catalog no. GTX 627408) or anti-vinculin (VCL; 1:20,000, Sigma-Aldrich, catalog no. V9131).

Auditory brainstem responses

ABR thresholds were recorded using the Intelligent Hearing Systems Smart EP program (IHS, Miami, FL). Animals were anesthetized as described above and kept warm on a heating pad (37°C). Needle electrodes were placed on the vertex (+), behind the left ear (−), and on the opposite ear (ground). Tone bursts were presented at 4, 8, 16, and 32 kHz, with a duration of 500 μs using a high-frequency transducer. The recording was carried out using a total gain equal to 100 K and using 100 Hz and 15 kHz settings for the high- and low-pass filters. A minimum of 128 sweeps was presented at 90 dB sound pressure level (SPL). The SPL was decreased in 10-dB steps. Near the threshold level, 5-dB SPL steps using up to 1,024 presentations were carried out at each frequency. The threshold was defined as the SPL at which at least one of the waves could be identified in two or more repetitions of the recording. The pre-operative threshold was measured in P16 animals before the first operation, and the final post-operative threshold was measured before sacrificing the animals.

Histopathology

Mice were anesthetized with intraperitoneal applications of phenobarbital (585 mg/kg) and phenytoin sodium (75 mg/kg)

(Beuthanasia-D Special, Schering-Plough Animal Health, Union, NJ, USA) and sacrificed via intracardiac perfusion with 4% paraformaldehyde in PBS. The temporal bones were removed and trimmed. The staples was removed, and the round window was opened with a needle. The temporal bones were postfixed overnight in 4% paraformaldehyde in PBS at 4°C. After rinsing in PBS three times for 30 min, the temporal bones were decalcified in 10% EDTA for 48 h. The decalcified otic capsule was carefully removed, and the organ of Corti was dissected away from the modiolus. The tissue was then incubated in PBS + 0.1% Triton X-100 for 10 min, followed by staining with phalloidin-FITC (1:80, Abcam, catalog no. ab235137) in PBS + 0.1% Triton X-100 for 20 min at room temperature. The tissue was washed three times for 10 min in PBS and mounted in Vectashield Plus mounting medium (Vector Labs, Newark, CA, USA).

Statistical analyses

The data are represented as mean ± SD and were analyzed with GraphPad Prism 5 software (GraphPad, La Jolla, CA, USA). To compare two groups (Figure 1), an unpaired, two-tailed t test was performed. In contrast, multiple groups were analyzed by one-way ANOVA together with Dunnett's post hoc test. A $p \leq 0.05$ (*) was considered statistically significant, $p \leq 0.01$ (**) was considered very significant, and $p \leq 0.001$ (***) was considered extremely significant. Each experiment's sample size (n) was specified in the respective figure legend.

DATA AND CODE AVAILABILITY

All of the data are available in the main text or the supplemental information.

SUPPLEMENTAL INFORMATION

Supplemental information can be found online at https://doi.org/10.1016/j.omtn.2024.102157.

ACKNOWLEDGMENTS

The authors are grateful to Girmay Asgedom and Thomas Neumann for technical support. We thank Teng Cheong Ha for kindly contributing the cDNA of *Bcl-xL*, Federico Kalinec (House Ear Institute, Los Angeles, CA, USA) for providing the HEI-OC1 cells, Francis Rousset and Pascal Senn (University of Geneva, Geneva, Switzerland) for supplying the phoenix auditory neuroprogenitor cells, Falk Büttner (Hannover Medical School, Hannover, Germany) for providing the heparan sulfate, and Thomas J. Hope (Northwestern University, Chicago, IL, USA) for supplying the pRSV.Rev expression plasmid. The graphical abstract was created using BioRender.com. This work received funding from the European Research Council under grant agreements nos. 819531 and 101082064.

AUTHOR CONTRIBUTIONS

Conceptualization, A.S., M. Galla, H.S., J.W.S., and M.M. Methodology, L.N., H.S., M. Galla, and A.S. Investigation, L.N., H.S., P.H., B.R., J.H., and M. Goblet. Resources, A.S., H.S., and A.W. Writing – original draft, L.N., M. Galla, and A.S. Visualization, L.N. and M. Galla. Supervision, M. Galla and A.S. Funding acquisition, A.S.

DECLARATION OF INTERESTS

J.W.S., M.M., A.W., A.S., and H.S. have submitted patent applications for LV gene therapy for the inner ear.

REFERENCES

1. Müller, U., and Barr-Gillespie, P.G. (2015). New treatment options for hearing loss. Nat. Rev. Drug Discov. *14*, 346–365. https://doi.org/10.1038/nrd4533.
2. Cruickshanks, K.J., Tweed, T.S., Wiley, T.L., Klein, B.E.K., Klein, R., Chappell, R., Nondahl, D.M., and Dalton, D.S. (2003). The 5-year incidence and progression of hearing loss: The epidemiology of hearing loss study. Arch. Otolaryngol. Head Neck Surg. *129*, 1041–1046. https://doi.org/10.1001/archotol.129.10.1041.
3. Ding, T., Yan, A., and Liu, K. (2019). What is noise-induced hearing loss? Br. J. Hosp. Med. *80*, 525–529. https://doi.org/10.12968/hmed.2019.80.9.525.
4. Lanvers-Kaminsky, C., Zehnhoff-Dinnesen, A.A., Parfitt, R., and Ciarimboli, G. (2017). Drug-induced ototoxicity: Mechanisms, pharmacogenetics, and protective strategies. Clin. Pharmacol. Ther. *101*, 491–500. https://doi.org/10.1002/cpt.603.
5. Kros, C.J., and Steyger, P.S. (2019). Aminoglycoside- and cisplatin-induced ototoxicity: Mechanisms and otoprotective strategies. Cold Spring Harb. Perspect. Med. *9*, a033548. https://doi.org/10.1101/cshperspect.a033548.
6. Tew, W.P., and Fleming, G.F. (2015). Treatment of ovarian cancer in the older woman. Gynecol. Oncol. *136*, 136–142. https://doi.org/10.1016/j.ygyno.2014.10.028.
7. Boer, H., Proost, J.H., Nuver, J., Bunskoek, S., Gietema, J.Q., Geubels, B.M., Altena, R., Zwart, N., Oosting, S.F., Vonk, J.M., et al. (2015). Long-term exposure to circulating platinum is associated with late effects of treatment in testicular cancer survivors. Ann. Oncol. *26*, 2305–2310. https://doi.org/10.1093/annonc/mdv369.
8. Strojan, P., Vermorken, J.B., Beitler, J.J., Saba, N.F., Haigentz, M., Bossi, P., Worden, F.P., Langendijk, J.A., Eisbruch, A., Mendenhall, W.M., et al. (2016). Cumulative cisplatin dose in concurrent chemoradiotherapy for head and neck cancer: A systematic review. Head Neck *38*, E2151–E2158. https://doi.org/10.1002/hed.24026.
9. Rybak, L.P., Mukherjea, D., Jajoo, S., and Ramkumar, V. (2009). Cisplatin ototoxicity and protection: Clinical and experimental Studies. Tohoku J. Exp. Med. *219*, 177–186. https://doi.org/10.1620/tjem.219.177.
10. Dasari, S., and Tchounwou, P.B. (2014). Cisplatin in cancer therapy: Molecular mechanisms of action. Eur. J. Pharmacol. *740*, 364–378. https://doi.org/10.1016/j.ejphar.2014.07.025.
11. Rybak, L.P., Mukherjea, D., Jajoo, S., and Ramkumar, V. (2009). Cisplatin Ototoxicity and Protection: Clinical and Experimental Studies *219*, 177–186. https://doi.org/10.1620/tjem.219.177.
12. Chirtes, F., and Albu, S. (2014). Prevention and restoration of hearing loss associated with the use of cisplatin. BioMed Res. Int. *2014*, 925485. https://doi.org/10.1155/2014/925485.
13. García-Berrocal, J.R., Nevado, J., Ramírez-Camacho, R., Sanz, R., González-García, J.A., Sánchez-Rodríguez, C., Cantos, B., España, P., Verdaguer, J.M., and Trinidad Cabezas, A. (2007). The anticancer drug cisplatin induces an intrinsic apoptotic pathway inside the inner ear. Br. J. Pharmacol. *152*, 1012–1020. https://doi.org/10.1038/sj.bjp.0707405.
14. Brock, P.R., Knight, K.R., Freyer, D.R., Campbell, K.C.M., Steyger, P.S., Blakley, B.W., Rassekh, S.R., Chang, K.W., Fligor, B.J., Rajput, K., et al. (2012). Platinum-induced ototoxicity in children: A consensus review on mechanisms, predisposition, and protection, including a new International Society of Pediatric Oncology Boston ototoxicity scale. J. Clin. Oncol. *30*, 2408–2417. https://doi.org/10.1200/JCO.2011.39.1110.
15. Dammeyer, P., Hellberg, V., Wallin, I., Laurell, G., Shoshan, M., Ehrsson, H., Arnér, E.S.J., and Kirkegaard, M. (2014). Cisplatin and oxaliplatin are toxic to cochlear outer hair cells and both target thioredoxin reductase in organ of Corti cultures. Acta Otolaryngol. *134*, 448–454. https://doi.org/10.3109/00016489.2013.879740.
16. Guthrie, O.W., Li-Korotky, H.S., Durrant, J.D., and Balaban, C. (2008). Cisplatin induces cytoplasmic to nuclear translocation of nucleotide excision repair factors among spiral ganglion neurons. Hear. Res. *239*, 79–91. https://doi.org/10.1016/j.heares.2008.01.013.

17. Lee, J.E., Nakagawa, T., Kita, T., Kim, T.S., Iguchi, F., Endo, T., Shiga, A., Lee, S.H., and Ito, J. (2004). Mechanisms of apoptosis induced by cisplatin in marginal cells in mouse stria vascularis. ORL (Oto-Rhino-Laryngol.) (Basel) *66*, 111–118. https://doi.org/10.1159/000079329.

18. Kleih, M., Böpple, K., Dong, M., Gaißler, A., Heine, S., Olayioye, M.A., Aulitzky, W.E., and Essmann, F. (2019). Direct impact of cisplatin on mitochondria induces ROS production that dictates cell fate of ovarian cancer cells. Cell Death Dis. *10*, 851. https://doi.org/10.1038/s41419-019-2081-4.

19. Itoh, T., Terazawa, R., Kojima, K., Nakane, K., Deguchi, T., Ando, M., Tsukamasa, Y., Ito, M., and Nozawa, Y. (2011). Cisplatin induces production of reactive oxygen species via NADPH oxidase activation in human prostate cancer cells. Free Radic. Res. *45*, 1033–1039. https://doi.org/10.3109/10715762.2011.591391.

20. Jordan, P., and Carmo-Fonseca, M. (2000). Molecular mechanisms involved in cisplatin cytotoxicity. Cell. Mol. Life Sci. *57*, 1229–1235. https://doi.org/10.1007/pl00000762.

21. Davies, K.J. (2000). Oxidative stress, antioxidant defenses, and damage removal, repair, and replacement systems. IUBMB Life *50*, 279–289. https://doi.org/10.1080/713803728.

22. Kartalou, M., and Essigmann, J.M. (2001). Mechanisms of resistance to cisplatin. Mutat. Res. *478*, 23–43. https://doi.org/10.1016/s0027-5107(01)00141-5.

23. Furness, D.N. (2015). Molecular basis of hair cell loss. Cell Tissue Res. *361*, 387–399. https://doi.org/10.1007/s00441-015-2113-z.

24. Brock, P.R., Maibach, R., Childs, M., Rajput, K., Roebuck, D., Sullivan, M.J., Laithier, V., Ronghe, M., Dall'Igna, P., Hiyama, E., et al. (2018). Sodium thiosulfate for protection from cisplatin-induced hearing loss. N. Engl. J. Med. *378*, 2376–2385. https://doi.org/10.1056/nejmoa1801109.

25. Wang, J., Lloyd Faulconbridge, R.V., Fetoni, A., Guitton, M.J., Pujol, R., and Puel, J.L. (2003). Local application of sodium thiosulfate prevents cisplatin-induced hearing loss in the guinea pig. Neuropharmacology *45*, 380–393. https://doi.org/10.1016/S0028-3908(03)00194-1.

26. Hill, G.W., Morest, D.K., and Parham, K. (2008). Cisplatin-induced ototoxicity: Effect of intratympanic dexamethasone injections. Otol. Neurotol. *29*, 1005–1011. https://doi.org/10.1097/MAO.0b013e31818599d5.

27. Murphy, D., and Daniel, S.J. (2011). Intratympanic dexamethasone to prevent cisplatin ototoxicity: A guinea pig model. Otolaryngol. Head Neck Surg. *145*, 452–457. https://doi.org/10.1177/0194599811406673.

28. Hughes, A.L., Hussain, N., Pafford, R., and Parham, K. (2014). Dexamethasone otoprotection in a multidose cisplatin ototoxicity mouse model. Otolaryngol. Head Neck Surg. *150*, 115–120. https://doi.org/10.1177/0194599813511948.

29. Wang, J., Ladrech, S., Pujol, R., Brabet, P., van de Water, T.R., and Puel, J.-L. (2004). Caspase inhibitors, but not c-Jun NH 2-terminal kinase inhibitor treatment, prevent cisplatin-induced hearing loss. Cancer Res. *64*, 9217–9224. https://doi.org/10.1158/0008-5472.CAN-04-1581.

30. Freyer, D.R., Chen, L., Krailo, M.D., Knight, K., Villaluna, D., Bliss, B., Pollock, B.H., Ramdas, J., Lange, B., Van Hoff, D., et al. (2017). Effects of sodium thiosulfate versus observation on development of cisplatin-induced hearing loss in children with cancer (ACCL0431): a multicentre, randomised, controlled, open-label, phase 3 trial. Lancet Oncol. *18*, 63–74. https://doi.org/10.1016/S1470-2045(16)30625-8.

31. Videhult, P., Laurell, G., Wallin, I., and Ehrsson, H. (2006). Kinetics of cisplatin and its monohydrated complex with sulfur-containing compounds designed for local otoprotective administration. Exp. Biol. Med. *231*, 1638–1645. https://doi.org/10.1177/153537020623101009.

32. Van den Berg, J.H., Beijnen, J.H., Balm, A.J.M., and Schellens, J.H.M. (2006). Future opportunities in preventing cisplatin induced ototoxicity. Cancer Treat Rev. *32*, 390–397. https://doi.org/10.1016/j.ctrv.2006.04.011.

33. Nguyen, T.N., and Park, J.S. (2023). Intratympanic drug delivery systems to treat inner ear impairments. J. Pharm. Investig. *53*, 93–118. https://doi.org/10.1007/s40005-022-00586-8.

34. Yildiz, E., Gadenstaetter, A.J., Gerlitz, M., Landegger, L.D., Liepins, R., Nieratschker, M., Glueckert, R., Staecker, H., Honeder, C., and Arnoldner, C. (2023). Investigation of inner ear drug delivery with a cochlear catheter in piglets as a representative model for human cochlear pharmacokinetics. Front. Pharmacol. *14*, 1062379. https://doi.org/10.3389/fphar.2023.1062379.

35. Gehrke, M., Sircoglou, J., Gnansia, D., Tourrel, G., Willart, J.F., Danede, F., Lacante, E., Vincent, C., Siepmann, F., and Siepmann, J. (2016). Ear cubes for local controlled drug delivery to the inner ear. Int. J. Pharm. *509*, 85–94. https://doi.org/10.1016/j.ijpharm.2016.04.003.

36. Araya, C.E., Fennell, R.S., Neiberger, R.E., and Dharnidharka, V.R. (2006). Sodium thiosulfate treatment for calcific uremic arteriolopathy in children and young adults. Clin. J. Am. Soc. Nephrol. *1*, 1161–1166. https://doi.org/10.2215/CJN.01520506.

37. O'sullivan, B.T., Cutler, D.J., Hunt, G.E., Walters, C., Johnson, G.F., and Caterson, I.D. (1997). Pharmacokinetics of dexamethasone and its relationship to dexamethasone suppression outcome in depressed patients and healthy subjects. Biol. Psychiatry *41*, 574–584. https://doi.org/10.1016/s0006-3223(96)00094-7.

38. Cronin, J., Zhang, X.-Y., and Reiser, J. (2005). Altering the tropism of lentiviral vectors through pseudotyping. Curr. Gene Ther. *5*, 387–398. https://doi.org/10.2174/1566523054546224.

39. Morgan, M., Schott, J.W., Rossi, A., Landgraf, C., Warnecke, A., Staecker, H., Lesinski-Schiedat, A., Schlegelberger, B., Büning, H., Auber, B., and Schambach, A. (2020). Gene therapy as a possible option to treat hereditary hearing loss. Med. Genet. *32*, 149–159. https://doi.org/10.1515/medgen-2020-2021.

40. Pietola, L., Aarnisalo, A.A., Joensuu, J., Pellinen, R., Wahlfors, J., and Jero, J. (2008). HOX-GFP and WOX-GFP lentivirus vectors for inner ear gene transfer. Acta Otolaryngol. *128*, 613–620. https://doi.org/10.1080/00016480701663409.

41. Pan, S., Wan, J., Liu, S., Zhang, S., Xiong, H., Zhou, J., Xiong, W., Yu, K., and Fu, Y. (2013). Lentivirus carrying the Atoh1 gene infects normal rat cochlea. Neural Regen. Res. *8*, 1551–1559. https://doi.org/10.3969/j.issn.1673-5374.2013.17.002.

42. Kalinec, G.M., Webster, P., Lim, D.J., and Kalinec, F. (2003). A cochlear cell line as an *in vitro* system for drug ototoxicity screening. Audiol. Neurootol. *8*, 177–189. https://doi.org/10.1159/000071059.

43. Kalinec, G., Thein, P., Park, C., and Kalinec, F. (2016). HEI-OC1 cells as a model for investigating drug cytotoxicity. Hear. Res. *335*, 105–117. https://doi.org/10.1016/j.heares.2016.02.019.

44. Im, G.J., Chang, J.W., Choi, J., Chae, S.W., Ko, E.J., and Jung, H.H. (2010). Protective effect of Korean red ginseng extract on cisplatin ototoxicity in HEI-OC1 auditory cells. Phytother Res. *24*, 614–621. https://doi.org/10.1002/ptr.3082.

45. Yin, H., Sun, G., Yang, Q., Chen, C., Qi, Q., Wang, H., and Li, J. (2017). NLRX1 accelerates cisplatin-induced ototoxity in HEI-OC1 cells via promoting generation of ROS and activation of JNK signaling pathway. Sci. Rep. *7*, 44311. https://doi.org/10.1038/srep44311.

46. Li, H., Song, Y., He, Z., Chen, X., Wu, X., Li, X., Bai, X., Liu, W., Li, B., Wang, S., et al. (2018). Meclofenamic acid reduces reactive oxygen species accumulation and apoptosis, inhibits excessive autophagy, and protects hair cell-like HEI-OC1 cells from cisplatin-induced damage. Front. Cell. Neurosci. *12*, 139. https://doi.org/10.3389/fncel.2018.00139.

47. Hellberg, V., Wallin, I., Ehrsson, H., and Laurell, G. (2013). Cochlear pharmacokinetics of cisplatin: An *in vivo* study in the guinea pig. Laryngoscope *123*, 3172–3177. https://doi.org/10.1002/lary.24235.

48. Mcalpine, D., and Johnstone, B.M. (1990). The ototoxic mechanism of cisplatin. Hear. Res. *47*, 191–203. https://doi.org/10.1019/0379-5955(90)90151-e.

49. Rybak, L.P., Whitworth, C., and Somani, S. (1999). Application of antioxidants and other agents to prevent cisplatin ototoxicity. Laryngoscope *109*, 1740–1744. https://doi.org/10.1097/00005537-199911000-00003.

50. Kopke, R.D., Liu, W., Gabaizadeh, R., Jacono, A., Feghali, J., Spray, D., Garcia, P., Steinman, H., Malgrange, B., Ruben, R.J., et al. (1997). Use of organotypic cultures of Corti's organ to study the protective effects of antioxidant molecules on cisplatin-induced damage of auditory hair cells. Am. J. Otol. *18*, 559–571.

51. Jiang, M., Qi, L., Li, L., and Li, Y. (2020). The caspase-3/GSDME signal pathway as a switch between apoptosis and pyroptosis in cancer. Cell Death Discov. *6*, 112. https://doi.org/10.1038/s41420-020-00349-0.

52. Vermes, I., Haanen, C., Steffens-Nakken, H., and Reutelingsperger, C. (1995). A novel assay for apoptosis flow cytometric detection of phosphatidylserine early

apoptotic cells using fluorescein labelled expression on Annexin V. J. Immunol. Methods *184*, 39–51. https://doi.org/10.1016/0022-1759(95)00072-i.

53. Rybak, L.P., Husain, K., Morris, C., Whitworth, C., and Somani, S. (2000). Effect of protective agents against cisplatin ototoxicity. Am. J. Otol. *21*, 513–520.

54. Kil, J., Pierce, C., Tran, H., Gu, R., and Lynch, E.D. (2007). Ebselen treatment reduces noise induced hearing loss via the mimicry and induction of glutathione peroxidase. Hear. Res. *226*, 44–51. https://doi.org/10.1016/j.heares.2006.08.006.

55. Johnson, K.R., Yu, H., Ding, D., Jiang, H., Gagnon, L.H., and Salvi, R.J. (2010). Separate and combined effects of Sod1 and Cdh23 mutations on age-related hearing loss and cochlear pathology in C57BL/6J mice. Hear. Res. *268*, 85–92. https://doi.org/10.1016/j.heares.2010.05.002.

56. Goyal, M.M., and Basak, A. (2010). Human catalase: Looking for complete identity. Protein Cell *1*, 888–897. https://doi.org/10.1007/s13238-010-0113-z.

57. Brigelius-Flohé, R., and Maiorino, M. (2013). Glutathione peroxidases. Biochim. Biophys. Acta *1830*, 3289–3303. https://doi.org/10.1016/j.bbagen.2012.11.020.

58. Ceckova, M., Vackova, Z., Radilova, H., Libra, A., Buncek, M., and Staud, F. (2008). Effect of ABCG2 on cytotoxicity of platinum drugs: Interference of EGFP. Toxicol. Vitro *22*, 1846–1852. https://doi.org/10.1016/j.tiv.2008.09.001.

59. Antonsson, B., and Martinou, J.C. (2000). The Bcl-2 protein family. Exp. Cell Res. *256*, 50–57. https://doi.org/10.1006/excr.2000.4839.

60. Reed, J.C. (1994). Bcl-2 and the regulation of programmed cell death. J. Cell Biol. *124*, 1–6.

61. Boise, L.H., González-García, M., Postema, C.E., Ding, L., Lindsten, T., Turka, L.A., Mao, X., Nuñez, G., and Thompson, C.B. (1993). Bcl-xl, a bcl-2-related gene that functions as a dominant regulator of apoptotic cell death. Cell *74*, 597–608. https://doi.org/10.1016/0092-8674(93)90508-n.

62. Czabotar, P.E., and Garcia-Saez, A.J. (2023). Mechanisms of BCL-2 family proteins in mitochondrial apoptosis. Nat. Rev. Mol. Cell Biol. *24*, 732–748. https://doi.org/10.1038/s41580-023-00629-4.

63. Eskes, R., Desagher, S., Antonsson, B., and Martinou, J.-C. (2000). Bid induces the oligomerization and insertion of Bax into the outer mitochondrial membrane. Mol. Cell Biol. *20*, 929–935. https://doi.org/10.1128/MCB.20.3.929-935.2000.

64. Wei, M.C., Lindsten, T., Mootha, V.K., Weiler, S., Gross, A., Ashiya, M., Thompson, C.B., and Korsmeyer, S.J. (2000). tBID, a membrane-targeted death ligand, oligomerizes BAK to release cytochrome c. Genes Dev. *14*, 2060–2071.

65. González-García, M., Pérez-Ballestero, R., Ding, L., Duan, L., Boise, L.H., Thompson, C.B., and Núñez, G. (1994). bcl-xL is the major bcl-x mRNA form expressed during murine development and its product localizes to mitochondria. Development *120*, 3033–3042. https://doi.org/10.1242/dev.120.10.3033.

66. Rousset, F., Kokje, V.B.C., Sipione, R., Schmidbauer, D., Nacher-Soler, G., Ilmjärv, S., Coelho, M., Fink, S., Voruz, F., El Chemaly, A., et al. (2020). Intrinsically self-renewing neuroprogenitors from the A/J mouse spiral ganglion as virtually unlimited source of mature auditory neurons. Front. Cell. Neurosci. *14*. https://doi.org/10.3389/fncel.2020.599152.

67. Rousset, F., Schmidbauer, D., Fink, S., Adel, Y., Obexer, B., Müller, M., Glueckert, R., Löwenheim, H., and Senn, P. (2022). Phoenix auditory neurons as 3R cell model for high throughput screening of neurogenic compounds. Hear. Res. *414*, 108391. https://doi.org/10.1016/j.heares.2021.108391.

68. Schmidt, N., Schulze, J., Warwas, D.P., Ehlert, N., Lenarz, T., Warnecke, A., and Behrens, P. (2018). Long-term delivery of brain-derived neurotrophic factor (BDNF) from nanoporous silica nanoparticles improves the survival of spiral ganglion neurons *in vitro*. PLoS One *13*, e0194778. https://doi.org/10.1371/journal.pone.0194778.

69. Kisselbach, L., Merges, M., Bossie, A., and Boyd, A. (2009). CD90 expression on human primary cells and elimination of contaminating fibroblasts from cell cultures. Cytotechnology *59*, 31–44. https://doi.org/10.1007/s10616-009-9190-3.

70. Locher, H., de Groot, J.C.M.J., van Iperen, L., Huisman, M.A., Frijns, J.H.M., and Chuva De Sousa Lopes, S.M. (2014). Distribution and development of peripheral glial cells in the human fetal cochlea. PLoS One *9*, e88066. https://doi.org/10.1371/journal.pone.0088066.

71. Li, C., Li, X., Bi, Z., Sugino, K., Wang, G., Zhu, T., and Liu, Z. (2020). Comprehensive transcriptome analysis of cochlear spiral ganglion neurons at multiple ages. Elife *9*, e50491. https://doi.org/10.7554/eLife.50491.

72. Sauer, R., Schrott, K.M., Dunst, J., Thiel, H.J., Hermanek, P., and Bornhof, C. (1988). Preliminary results of treatment of invasive bladder carcinoma with radiotherapy and cisplatin. Int. J. Radiat. Oncol. Biol. Phys. *15*, 871–875. https://doi.org/10.1016/0360-3016(88)90120-4.

73. Berg, A.L., Spitzer, J.B., and Garvin, J.H., Jr. (1999). Ototoxic impact of cisplatin in pediatric oncology patients. Laryngoscope *109*, 1806–1814. https://doi.org/10.1097/00005537-199911000-00016.

74. Waters, G.S., Ahmad, M., Katsarkas, A., Stanimir, G., and Mckay, J. (1991). Otology and neurotology ototoxicity due to cis-diamminedichloro-platinum in the treatment of ovarian cancer: Influence of dosage and schedule of administration. Ear Hear. *12*, 91–102. https://doi.org/10.1097/00003446-199104000-00003.

75. Laurell, G., Beskow, C., Frankendal, B., and Borg, E. (1996). Cisplatin administration to gynecologic cancer patients. Long-term effects on hearing. Cancer *78*, 1798–1804.

76. Wang, X., Zhou, Y., Wang, D., Wang, Y., Zhou, Z., Ma, X., Liu, X., and Dong, Y. (2023). Cisplatin-induced ototoxicity: From signaling network to therapeutic targets. Biomed. Pharmacother. *157*, 114045. https://doi.org/10.1016/j.biopha.2022.114045.

77. Paken, J., Govender, C.D., Pillay, M., and Sewram, V. (2019). A review of cisplatin-associated ototoxicity. Semin. Hear. *40*, 108–121. https://doi.org/10.1055/s-0039-1684041.

78. Rademaker-Lakhai, J.M., Crul, M., Zuur, L., Baas, P., Beijnen, J.H., Simis, Y.J.W., van Zandwijk, N., and Schellens, J.H.M. (2006). Relationship between cisplatin administration and the development of ototoxicity. J. Clin. Oncol. *24*, 918–924. https://doi.org/10.1200/JCO.2006.10.077.

79. Zelko, I.N., Mariani, T.J., and Folz, R.J. (2002). Superoxide dismutase multigene family: a comparison of the CuZn-SOD (SOD1), Mn-SOD (SOD2), and EC-SOD (SOD3) gene structures, evolution, and expression. Free Radic. Biol. Med. *33*, 337–349. https://doi.org/10.1016/s0891-5849(02)00905-x.

80. Kawamoto, K., Sha, S.H., Minoda, R., Izumikawa, M., Kuriyama, H., Schacht, J., and Raphael, Y. (2004). Antioxidant gene therapy can protect hearing and hair cells from ototoxicity. Mol. Ther. *9*, 173–181. https://doi.org/10.1016/j.ymthe.2003.11.020.

81. Ohlemiller, K.K., Mcfadden, S.L., Ding, D.-L., Flood, D.G., Reaume, A.G., Hoffman, E.K., Scott, R.W., Wright, J.S., Putcha, G.V., and Salvi, R.J. (1999). Targeted deletion of the cytosolic Cu/Zn-superoxide dismutase gene (Sod1) increases susceptibility to noise-induced hearing loss. Audiol. Neurootol. *4*, 237–246. https://doi.org/10.1159/000013847.

82. Kim, S.J., Hur, J.H., Park, C., Kim, H.J., Oh, G.S., Lee, J.N., Yoo, S.J., Choe, S.K., So, H.S., Lim, D.J., et al. (2015). Bucillamine prevents cisplatin-induced ototoxicity through induction of glutathione and antioxidant genes. Exp. Mol. Med. *47*. https://doi.org/10.1038/emm.2014.112.

83. Cooper, L.B., Chan, D.K., Roediger, F.C., Shaffer, B.R., Fraser, J.F., Musatov, S., Selesnick, S.H., and Kaplitt, M.G. (2006). AAV-mediated delivery of the caspase inhibitor XIAP protects against cisplatin ototoxicity. Otol. Neurotol. *27*, 484–490. https://doi.org/10.1097/01.mao.0000202647.19355.6a.

84. Staecker, H., Liu, W., Malgrange, B., Lefebvre, P.P., and van de Water, T.R. (2007). Vector-mediated delivery of bcl-2 prevents degeneration of auditory hair cells and neurons after injury. ORL. J. Otorhinolaryngol. Relat. Spec. *69*, 43–50. https://doi.org/10.1159/000096716.

85. Schott, J.W., Huang, P., Morgan, M., Nelson-Brantley, J., Koehler, A., Renslo, B., Büning, H., Warnecke, A., Schambach, A., and Staecker, H. (2023). Third-generation lentiviral gene therapy rescues function in a mouse model of Usher 1B. Mol. Ther. *31*, 3502–3519. https://doi.org/10.1016/j.ymthe.2023.10.018.

86. Craggs, T.D. (2009). Green fluorescent protein: Structure, folding and chromophore maturation. Chem. Soc. Rev. *38*, 2865–2875. https://doi.org/10.1039/b903641p.

87. Kumagai, A., Ando, R., Miyatake, H., Greimel, P., Kobayashi, T., Hirabayashi, Y., Shimogori, T., and Miyawaki, A. (2013). A bilirubin-inducible fluorescent protein from eel muscle. Cell *153*, 1602–1611. https://doi.org/10.1016/j.cell.2013.05.038.

88. Gossen, M., and Bujard, H. (1992). Tight control of gene expression in mammalian cells by tetracycline-responsive promoters. Proc. Natl. Acad. Sci. USA *89*, 5547–5551. https://doi.org/10.1073/pnas.89.12.5547.

89. Zhou, X., Vink, M., Klaver, B., Berkhout, B., and Das, A.T. (2006). Optimization of the Tet-On system for regulated gene expression through viral evolution. Gene Ther. *13*, 1382–1390. https://doi.org/10.1038/sj.gt.3302780.

90. Kallunki, T., Barisic, M., Jäättelä, M., and Liu, B. (2019). How to choose the right inducible gene expression system for Mammalian studies? Cells *8*, 796. https://doi.org/10.3390/cells8080796.

91. Dohmen, R.J., Wu, P., and Varshavsky, A. (1994). Heat-inducible degron: a method for constructing temperature-sensitive mutants. Science *263*, 1273–1276. https://doi.org/10.1126/science.8122109.

92. Johnston, J.A., Johnson, E.S., Waller, P.R., and Varshavsky, A. (1995). Methotrexate inhibits proteolysis of dihydrofolate reductase by the N-end rule pathway. J. Biol. Chem. *270*, 8172–8178. https://doi.org/10.1074/jbc.270.14.8172.

93. Peng, H., Chau, V.Q., Phetsang, W., Sebastian, R.M., Stone, M.R.L., Datta, S., Renwick, M., Tamer, Y.T., Toprak, E., Koh, A.Y., et al. (2019). Non-antibiotic Small-Molecule Regulation of DHFR-Based Destabilizing Domains *In Vivo*. Mol. Ther. Methods Clin. Dev. *15*, 27–39. https://doi.org/10.1016/j.omtm.2019.08.002.

94. Boëda, B., Weil, D., and Petit, C. (2001). A specific promoter of the sensory cells of the inner ear defined by transgenesis. Hum. Mol. Genet. *10*, 1581–1589. https://doi.org/10.1093/hmg/10.15.1581.

95. Hioki, H., Kameda, H., Nakamura, H., Okunomiya, T., Ohira, K., Nakamura, K., Kuroda, M., Furuta, T., and Kaneko, T. (2007). Efficient gene transduction of neurons by lentivirus with enhanced neuron-specific promoters. Gene Ther. *14*, 872–882. https://doi.org/10.1038/sj.gt.3302924.

96. Liu, D., and Fischer, I. (1996). Two alternative promoters direct neuron-specific expression of the rat microtubule-associated protein 1B gene. J. Neurosci. *16*, 5026–5036. https://doi.org/10.1523/JNEUROSCI.16-16-05026.1996.

97. Wefstaedt, P., Scheper, V., Lenarz, T., and Stöver, T. (2005). Brain-derived neurotrophic factor/glial cell line-derived neurotrophic factor survival effects on auditory neurons are not limited by dexamethasone. Neuroreport *16*, 2011–2014. https://doi.org/10.1097/00001756-200512190-00008.

98. Maass, J.C., Berndt, F.A., Cánovas, J., and Kukuljan, M. (2013). P27Kip1 knockdown induces proliferation in the organ of Corti in culture after efficient shRNA lentiviral transduction. J. Assoc. Res. Otolaryngol. *14*, 495–508. https://doi.org/10.1007/s10162-013-0383-2.

99. Schambach, A., Bohne, J., Chandra, S., Will, E., Margison, G.P., Williams, D.A., and Baum, C. (2006). Equal potency of gammaretroviral and lentiviral SIN vectors for expression of O6-methylguanine-DNA methyltransferase in hematopoietic cells. Mol. Ther. *13*, 391–400. https://doi.org/10.1016/j.ymthe.2005.08.012.

100. Yang, Y., Vanin, E.F., Whitt, M.A., Fornerod, M., Zwart, R., Schneiderman, R.D., Grosveld, G., and Nienhuis, A.W. (1995). Inducible, high-level production of infectious murine leukemia retroviral vector particles pseudotyped with vesicular stomatitis virus G envelope protein. Hum. Gene Ther. *6*, 1203–1213. https://doi.org/10.1089/hum.1995.6.9-1203.